

Contribution from the Department of Chemistry, University of Missouri—Rolla, Rolla, Missouri 65401

## Transition-Metal Complexes of Vitamin B<sub>6</sub> Related Compounds. 1. Synthesis and Electronic and Structural Properties of Several Divalent First-Row Transition-Metal Complexes of Pyridoxylideneamino Acids

JAMES T. WROBLESKI and GARY J. LONG\*

Received April 13, 1977

AIC702617

The synthesis and electronic and structural properties of 23 divalent first-row transition-metal complexes of pyridoxylidene-glycine, pyridoxylidenealanine, pyridoxylidenevaline, pyridoxylidene-phenylalanine, and pyridoxylidene-tryptophan are reported. The manganese(II), iron(II), cobalt(II), and nickel(II) complexes are of the type  $M(\text{HPLaa})_2 \cdot n\text{H}_2\text{O}$ , where HPLaa is the monoanion of a pyridoxylideneamino acid (Schiff base). The Cu(II) complexes are of the type  $\text{Cu}(\text{PLaa}) \cdot n\text{H}_2\text{O}$ , where PLaa is the dianion of a pyridoxylideneamino acid ligand. The Mn, Fe, Co, and Ni complexes formed with any one of these ligands are generally x-ray isomorphous. The high-spin Mn, Fe, Co, and Ni compounds all exhibit electronic spectral properties which are consistent with a distorted octahedral coordination geometry whereas these properties for the Cu(II) compounds are consistent with five-coordination. This five-coordination arises through intermolecular bridging via the pyridine nitrogen and 5'-hydroxymethyl groups in pyridoxal. The octahedral coordination involves the phenolate oxygen, the azomethine nitrogen, and the weakly bonded carboxylate oxygen in each Schiff base ligand. Infrared band assignments are given for the azomethine C=N stretch at ca.  $1660\text{ cm}^{-1}$ , the ring-carbon phenolate oxygen stretch at ca.  $1500\text{ cm}^{-1}$ , and the asymmetric carboxylate stretch at ca.  $1600\text{ cm}^{-1}$ . The low-frequency infrared spectrum shows only a single band near  $400\text{ cm}^{-1}$  which can be assigned to a metal-oxygen stretching absorption band. The  $^{57}\text{Fe}$  Mössbauer spectral parameters are typical of high-spin Fe(II) in a distorted octahedral ligand field. These results indicate that the pyridoxylideneamino acid ligands form, in general, coordination compounds different than the salicylideneamino acid ligands. This is consistent with the observation that the salicylideneamino acid complexes are not good vitamin B<sub>6</sub> model complexes. The relative effectiveness of  $\text{Zn}^{2+}$ ,  $\text{Ni}^{2+}$ , and  $\text{Co}^{2+}$  as catalysts in these reactions is explained in terms of their electronic and structural properties.

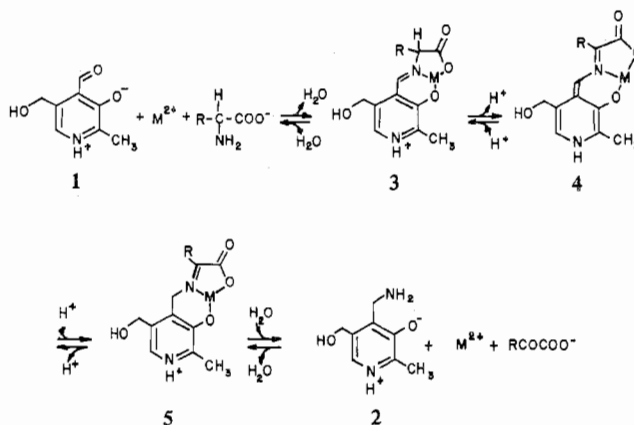
### Introduction

In 1939 Braunstein<sup>1</sup> and Cohen<sup>2</sup> discovered enzymatic transamination, the stoichiometry of which is given in reaction 1. In 1945 Snell<sup>3</sup> reported that pyridoxal (**1**) [3-hydroxy-amino acid<sub>1</sub> + keto acid<sub>2</sub>  $\rightleftharpoons$  keto acid<sub>1</sub> + amino acid<sub>2</sub> (1)

5-hydroxymethyl-2-methylpyridine-4-carboxaldehyde] catalyzed nonenzymatic transamination. More recently, Metzler et al.,<sup>4</sup> Guirard and Snell,<sup>5</sup> and Ikawa and Snell<sup>6</sup> reported the involvement of pyridoxal 5'-phosphate in several enzymatic transamination reactions. Others<sup>7-10</sup> showed that pyridoxal is catalytically involved in several decarboxylation, deamination, and racemization reactions. Much of this work was the topic of an international symposium<sup>11</sup> and an extensive review.<sup>12</sup>

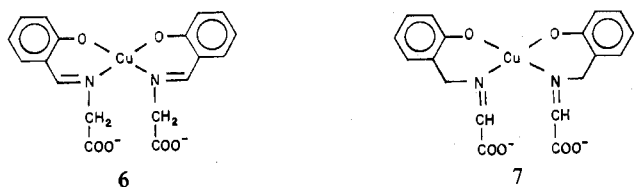
Metzler and Snell<sup>13</sup> studied the influence of both di- and trivalent metal ions on the reversible rates of transamination of pyridoxal with various amino acids. Longenecker and Snell<sup>14</sup> investigated the influence of metal ions on the rate of the transamination of pyridoxamine (**2**) with  $\alpha$ -ketoglutarate. These studies established that metal ions were catalytically efficient toward pyridoxal transamination in the order  $\text{Cu}^{2+} > \text{Al}^{3+} > \text{Fe}^{2+} > \text{Fe}^{3+} > \text{Zn}^{2+} > \text{Ni}^{2+} > \text{Co}^{2+}$ . Metzler et al.<sup>4</sup> extended the general mechanism of Braunstein<sup>15</sup> to account for the involvement of metal ions. This mechanism is shown in Scheme I. The imines **3** and **5** have been detected spectrophotometrically but direct evidence supporting the existence of intermediate **4** is lacking. Metzler and Snell<sup>13</sup> suggested that the metal ion stabilized the imines **3** and **5**, provided a planar conjugated system (via **4**), and increased the inductive effect away from the  $\alpha$ -carbon.<sup>12</sup> The work of Farago and Matthews<sup>16</sup> supported these suggestions and it is now believed that the metal ion does not kinetically affect the rate of formation of the Schiff base but rather serves as a trap for the preformed Schiff base. The metal complex **3** provides a planar structure which permits facile electron transfer via the extended  $\pi$ -orbital system. This hypothesis followed the observation of Pfeiffer et al.<sup>17</sup> who discovered that a solution of the aldimine complex **6** contained an equilibrium amount of the ketimine tautomer **7**.

### Scheme I



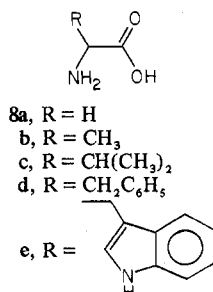
Prior to the experiments of Metzler and Snell,<sup>13</sup> Christensen and co-workers<sup>18,19</sup> isolated as crystalline solids several metal complexes of pyridoxylideneamino acids. Subsequently, Christensen extended the series of compounds and attempted an analysis of their acid-base properties and structures.<sup>20-22</sup> Baddiley<sup>23</sup> also reported the isolation of several of these compounds. More recently, Abbott and Martell,<sup>24,25</sup> Gansow and Holm,<sup>26,27</sup> and Martell and Eidson<sup>28</sup> have studied the  $\text{Al}^{3+}$  chelates of pyridoxylideneamino acids. Single-crystal x-ray diffraction studies of several metal complexes of these ligands have been reported.<sup>29-31</sup> Holm<sup>32</sup> has reviewed the literature covering the "vitamin B<sub>6</sub>" complexes.

Because very little was known about the electronic and structural properties of these important complexes which are implicated in several important model reactions, we decided to begin a systematic study of an extensive series of metal complexes of various pyridoxylideneamino acids. This paper describes our results for the Mn(II), Fe(II), Co(II), Ni(II), and Cu(II) complexes of pyridoxylidene-glycine, pyridoxylidenealanine, pyridoxylidenevaline, pyridoxylidene-phenylalanine, and pyridoxylidene-tryptophan. These five amino acids were selected because they provide a useful range of donor properties; namely, a gradual increase in ligand bulkiness and

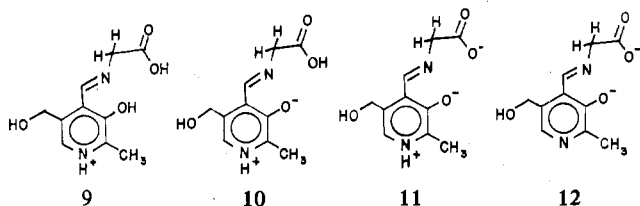


a significant variation in base strength. The first-row transition metals were selected because they would provide the most effective coordination chemistry probes into the electronic and magnetic properties of the complexes.

Certain abbreviations will be useful for the purpose of this paper. Thus, pyridoxal 1 is abbreviated H<sub>2</sub>PL, and  $\alpha$ -amino acid 8 is aa. By using this convention, the specific amino acids, in their dipolar ionic forms, are abbreviated as follows: glycine



(8a) is gly; alanine (8b) is ala; valine (8c) is val; phenylalanine (8d) is phe; tryptophan (8e) is trp. By using these abbreviations the monocation pyridoxylidenglycine (9) is H<sub>2</sub>PLgly<sup>+</sup>.



The zwitterionic compound 10 is H<sub>2</sub>PLgly. The monoanion 11 is HPLgly<sup>-</sup>. The dianion 12 is PLgly<sup>2-</sup>. Cahn-Ingold-Prelog notation is used to identify the absolute stereochemistry at asymmetric carbons.<sup>33</sup>

### Experimental Section

Pyridoxal hydrochloride was obtained from Sigma Chemical Co., St. Louis, Mo. The amino acids and metal salts were recrystallized prior to use. Pyridoxal free base was prepared by titrating a saturated aqueous solution of the hydrochloride with 2 N KOH. Infrared spectra were recorded on a Perkin-Elmer 180 spectrophotometer on samples in KBr or CsI disks and Nujol mulls. Electronic spectra of both solids and solutions were obtained on a Cary 14 spectrophotometer equipped with an Air Products AC-2 Joule-Thompson refrigerator operating on a hydrogen cycle.<sup>34</sup> The solid-state spectra were obtained by using samples dispersed in Kel-F 90 grease<sup>35</sup> or pressed in KBr pellets.<sup>36</sup> Complex spectral envelopes were resolved by using the bigaussian deconvolution scheme of Rakita et al.<sup>37</sup> Magnetic susceptibility data were obtained on polycrystalline samples on a standard Gouy or Faraday balance. The susceptibility standard was HgCo(NCS)<sub>4</sub>.<sup>38</sup> Diamagnetic corrections were made by using tables of Pascal's constants.<sup>39</sup> Iron Mössbauer spectra were obtained on polycrystalline samples by using a constant acceleration Austin Science Associates Mössbauer spectrometer which was calibrated with natural iron foil. The source was <sup>57</sup>Co(Cu) and was at room temperature for all experiments. Values of  $\sigma$ , the standard deviation, were calculated by using standard error propagation equations and the uncertainties in the least-squares computer fit of a parabola plus Lorentzians to the data and are given as value ( $\sigma$ ) in Table IV. X-ray powder diffraction patterns were obtained by the Straumanis technique by using nickel-filtered copper K $\alpha$  radiation ( $\lambda_{\text{mean}}$  1.5418 Å).

All metal analyses were performed in this laboratory. Manganese and zinc were analyzed by EDTA titrimetry by using Erichrome Black T as indicator. Iron was determined spectrophotometrically as the

1,10-phenanthroline complex. Cobalt was analyzed by atomic absorption. Nickel was determined gravimetrically as the dimethylglyoxime complex. Copper was determined iodometrically. The complexes were easily decomposed in dilute hydrochloric acid. Total amine was determined by the ninhydrin assay method.<sup>40</sup> Aldehyde was determined by the ethanolic method of Metzler and Snell.<sup>41</sup> The estimated standard deviation of the amine assay is  $\pm 2\%$  while that of the aldehyde assay is  $\pm 1\%$ . Carbon, hydrogen, and nitrogen elemental analyses were performed by Galbraith Laboratories, Inc., Knoxville, Tenn. The analytical data are given in Table I.<sup>42</sup>

**Bis(pyridoxylidenglycinate)iron(II).** Fe(HPLgly)<sub>2</sub> was prepared in Schlenk-type glassware under a constant flow of nitrogen. The system was charged with 50 mL of deoxygenated methanol and 25 mL of deoxygenated water. To this solvent was added 850 mg of H<sub>2</sub>PL free base (5 mmol) and 375 mg of glycine (5 mmol). The solution was immersed in an ice water bath and sufficient concentrated hydrochloric acid was added to make the solution approximately pH 5. During 30 min of stirring, the solution turned a dark yellow. To this solution was added 497 mg of FeCl<sub>2</sub>·4H<sub>2</sub>O (2.5 mmol) dissolved in 10 mL of deoxygenated methanol. The resulting green solution was freeze-dried leaving a dark green solid which was recrystallized from water. The recrystallization was carried out in a nitrogen-filled glovebag. An aliquot of the recrystallization mother liquor, which had been withdrawn from the glovebag, turned red within a few seconds when exposed to the air. The recrystallized compound was dried by passing a stream of nitrogen through the glovebag. The green material was homogeneous to chromatography on silica gel. Anal. Calcd for (FeC<sub>20</sub>H<sub>22</sub>N<sub>4</sub>O<sub>8</sub>) Fe, C, H, N: calcd, 11.11; found, 11.89.

In a subsequent experiment the mixed solvent above was replaced by 100 mL of deoxygenated water and the pH was adjusted to 8. Then the above procedure gave a green material which analyzed as the 6.5-hydrate. Anal. (FeC<sub>20</sub>H<sub>22</sub>N<sub>4</sub>O<sub>8</sub>·6.5H<sub>2</sub>O) Fe, C, H, N: calcd, 9.05; found, 7.62.

**Bis(pyridoxylidenglycinate)cobalt(II) Tetrahydrate.** Co(HPLgly)<sub>2</sub>·4H<sub>2</sub>O was prepared by combining 170 mg of H<sub>2</sub>PL free base (1 mmol), 75 mg of glycine (1 mmol), and 150 mg of Co(NH<sub>3</sub>)<sub>2</sub>·6H<sub>2</sub>O (0.5 mmol) in a solvent of 4 mL of ethanol and 15 mL of water. The resulting mixture was stirred at 0 °C for 12 h and then placed in a desiccator containing CaSO<sub>4</sub>. After 1 week red crystals formed in the remaining ethanol. The product was separated and dried in vacuo at room temperature to give a dark red crystalline material which analyzed as the tetrahydrate. Anal. (CoC<sub>20</sub>H<sub>22</sub>N<sub>4</sub>O<sub>8</sub>·4H<sub>2</sub>O) Co, C, H, N, amine.

**Bis(pyridoxylidenglycinate)nickel(II) Tetrahydrate.** Ni(HPLgly)<sub>2</sub>·4H<sub>2</sub>O was prepared in exactly the same manner as the cobalt complex above except that 120 mg of NiCl<sub>2</sub>·6H<sub>2</sub>O (0.5 mmol) was used. The product was a yellow-brown crystalline solid. Anal. (NiC<sub>20</sub>H<sub>22</sub>N<sub>4</sub>O<sub>8</sub>·4H<sub>2</sub>O) Ni, C, H, N, amine.

**Pyridoxylidenglycinatecopper(II) Dihydrate.** CuPLgly·2H<sub>2</sub>O was prepared by adding 500 mg of Cu(C<sub>2</sub>H<sub>3</sub>O<sub>2</sub>)<sub>2</sub>·2H<sub>2</sub>O (5.5 mmol) to a cold solution of 500 mg of sodium acetate, 300 mg of glycine (4 mmol), 350 mg of H<sub>2</sub>PL free base (2 mmol), and 40 mL of deionized water. This solution was stirred at 0 °C for 24 h. The green crystals which formed during this time were filtered and dried overnight at room temperature in vacuo. Anal. (CuC<sub>10</sub>H<sub>10</sub>N<sub>2</sub>O<sub>4</sub>·2H<sub>2</sub>O) Cu, C, H, N, amine; aldehyde: calcd, 46.78; found, 49.0.

**Bis(pyridoxylidene-2(S)-alaninato)manganese(II) Monohydrate.** Mn(HPL-2(S)-ala)<sub>2</sub>·H<sub>2</sub>O was prepared by adding 170 mg of H<sub>2</sub>PL free base (1 mmol), 89 mg of 2(S)-alanine (1 mmol), and 200 mg of MnCl<sub>2</sub>·4H<sub>2</sub>O to 25 mL of water containing 10 mL of methanol. Sufficient aqueous 2 N KOH was added to make the solution approximately pH 8. The mixture was stirred at room temperature for 2 days. The brown precipitate which had formed during this time was filtered and washed with methanol. This solid after drying over P<sub>2</sub>O<sub>5</sub> for 1 week was tan in color. Anal. (MnC<sub>24</sub>H<sub>26</sub>N<sub>4</sub>O<sub>8</sub>·H<sub>2</sub>O) Mn, C, H, N: calcd, 10.79; found, 9.92; aldehyde: calcd, 58.20; found, 52.0.

**Bis(pyridoxylidene-DL-alaninato)iron(II) Decahydrate.** Fe(HPL-DL-ala)<sub>2</sub>·10H<sub>2</sub>O was prepared in an N<sub>2</sub>-filled glovebox by adding 139 mg of FeSO<sub>4</sub>·7H<sub>2</sub>O (0.5 mmol) to a mixture containing 91 mg of DL-alanine (1.1 mmol), 170 mg of H<sub>2</sub>PL free base (1 mmol), 2 mL of deoxygenated water, and 25 mL of deoxygenated methanol. The resulting dark green solution was stirred at room temperature for several hours. The solution was evaporated to dryness by using a rotary evaporator. The residue was dissolved in 5 mL of methanol, filtered, and again evaporated to dryness. A small sample of the dried

material turned red when exposed to the air. The entire sample (about 300 mg) was dissolved in 1 mL of methanol and passed through a silica gel column previously equilibrated with 1 N aqueous sodium acetate. The sample separated into three bands. The bulk of the material appeared to be concentrated in the fastest moving band which was removed from the column. This green solution was evaporated to dryness yielding a dark green residue which was dried in vacuo for several hours. Anal. ( $\text{FeC}_{22}\text{H}_{26}\text{N}_4\text{O}_8 \cdot 10\text{H}_2\text{O}$ ) Fe, C, N; H: calcd, 6.78; found, 4.96.<sup>43</sup>

**Bis(pyridoxylidene-2(S)-alaninato)cobalt(II) Tetrahydrate.** Co(HPL-2(S)-ala)<sub>2</sub>·4H<sub>2</sub>O was prepared in the same way as Co(HPLgly)<sub>2</sub>·4H<sub>2</sub>O except that CoCl<sub>2</sub>·6H<sub>2</sub>O was used. The red crystalline product was washed with warm ethanol and dried at room temperature in vacuo for several hours. Anal. ( $\text{CoC}_{22}\text{H}_{26}\text{N}_4\text{O}_8 \cdot 4\text{H}_2\text{O}$ ) Co, C, H, N, amine.

**Bis(pyridoxylidene-2(S)-alaninato)nickel(II) Tetrahydrate.** Ni(HPL-2(S)-ala)<sub>2</sub>·4H<sub>2</sub>O was prepared by adding 1.67 g of H<sub>2</sub>PL free base (10 mmol), 0.910 g of 2(S)-alanine (10 mmol), 1.06 g of Ni(ClO<sub>4</sub>)<sub>2</sub>·6H<sub>2</sub>O (5 mmol), and one drop of concentrated perchloric acid to 100 mL of boiling methanol. After several minutes of stirring, a brown-yellow precipitate separated from solution. The solid was filtered, dried in air, and recrystallized from a large volume of hot water. Anal. ( $\text{NiC}_{22}\text{H}_{26}\text{N}_4\text{O}_8 \cdot 4\text{H}_2\text{O}$ ) Ni, C, H, N, amine.

**Pyridoxylidene-DL-alaninatocopper(II) Dihydrate.** CuPL-DL-ala·2H<sub>2</sub>O was prepared in the same way as CuPLgly·2H<sub>2</sub>O and isolated as a green powder. Anal. ( $\text{CuC}_{11}\text{H}_{12}\text{N}_2\text{O}_4 \cdot 2\text{H}_2\text{O}$ ) Cu, C, H, N; amine: calcd, 21.46; found, 25.0.

**Bis(pyridoxylidene-2(S)-valinato)manganese(II) Dihydrate.** Mn(HPL-2(S)-val)<sub>2</sub>·2H<sub>2</sub>O was prepared in the same way as the corresponding alanine complex. The material isolated in this case was a darker brown than Mn(HPL-2(S)-ala)<sub>2</sub>·2H<sub>2</sub>O. The valine compound turned to a much darker brown over a period of several months. Anal. ( $\text{MnC}_{26}\text{H}_{34}\text{N}_4\text{O}_8 \cdot 2\text{H}_2\text{O}$ ) C, H, N, amine; Mn: calcd, 8.84; found, 9.67.

**Bis(pyridoxylidene-DL-valinato)iron(II) Dihydrate.** Fe(HPL-DL-val)<sub>2</sub>·2H<sub>2</sub>O was prepared in the same way as the iron(II) complex of pyridoxylidene-DL-alanine. This compound, however, gave a single band on the silica gel column. The material was isolated as the dihydrate. Anal. ( $\text{FeC}_{26}\text{H}_{34}\text{N}_4\text{O}_8 \cdot 2\text{H}_2\text{O}$ ) Fe, C, H, N.

**Bis(pyridoxylidene-2(S)-valinato)cobalt(II) Tetrahydrate.** Co(HPL-2(S)-val)<sub>2</sub>·4H<sub>2</sub>O was prepared by dissolving 2.03 g of H<sub>2</sub>PL-HCl (10 mmol) in 80 mL of methanol containing 20 mL of water. The solution was placed in an ice bath and 15 mL of 0.67 N aqueous sodium hydroxide (10 mmol) slowly added. An aqueous solution of 1.19 g of CoCl<sub>2</sub>·6H<sub>2</sub>O was added with stirring. Finally, an aqueous suspension of 1.17 g of 2(S)-valine (5 mmol) was added dropwise. A red solution formed immediately. After several hours, the red crystals which had formed were filtered, washed with cold methanol, and dried at room temperature in air. Anal. ( $\text{CoC}_{26}\text{H}_{34}\text{N}_4\text{O}_8 \cdot 4\text{H}_2\text{O}$ ) Co, C, H, N, amine.

**Bis(pyridoxylidene-2(S)-valinato)nickel(II) Hydrate.** Ni(HPL-2(S)-val)<sub>2</sub>·3.5H<sub>2</sub>O was prepared by adding 22 mg of Ni metal (0.37 mmol) to hydrochloric acid, evaporating the solution, and recrystallizing the NiCl<sub>2</sub>·6H<sub>2</sub>O from cold water. The NiCl<sub>2</sub>·6H<sub>2</sub>O was added to 10 mL of methanol and cooled in an ice bath. A second solution was prepared by dissolving 128 mg of H<sub>2</sub>PL free base (0.77 mmol) and 90 mg of 2(S)-valine (0.77 mmol) in methanol containing sufficient 3 N aqueous KOH to bring about complete dissolution of the amino acid. The metal ion solution was added to the ligand solution. A brownish yellow solution resulted. This solution was stirred at room temperature for 12 h during which a brown precipitate formed. This powder was filtered, washed with methanol, and dried over CaSO<sub>4</sub> at room temperature. Anal. ( $\text{NiC}_{26}\text{H}_{34}\text{N}_4\text{O}_8 \cdot 3.5\text{H}_2\text{O}$ ) Ni, C, H, N; calcd, 8.52; found, 7.59.

**Pyridoxylidene-2(S)-valinatocopper(II).** CuPL-2(S)-val was prepared in the same way as the two preceding Cu(II) complexes. The compound was a dark green solid. Anal. ( $\text{CuC}_{13}\text{H}_{16}\text{N}_2\text{O}_4$ ) Cu, C, H, N, amine.

**Bis(pyridoxylidene-2(S)-phenylalaninato)iron(II) Pentadecahydrate.** Fe(HPL-2(S)-phe)<sub>2</sub>·15H<sub>2</sub>O was prepared in the same way as Fe(HPL-DL-ala)<sub>2</sub>·10H<sub>2</sub>O and was found to separate into two bands on the silica gel column. The band remaining at the origin of the column was discarded and the green band eluted with methanol. After removal of the solvent, the green compound was dried at room temperature. Anal. ( $\text{FeC}_{34}\text{H}_{34}\text{N}_4\text{O}_8 \cdot 15\text{H}_2\text{O}$ ) Fe, C, H; calcd, 6.77; found, 4.84; N: calcd, 5.87; found, 6.37.<sup>43</sup>

**Bis(pyridoxylidene-2(S)-phenylalaninato)cobalt(II) Tetrahydrate.** Co(HPL-2(S)-phe)<sub>2</sub>·4H<sub>2</sub>O was prepared in the same way as the corresponding valine complex and isolated as a red crystalline material. Anal. ( $\text{CoC}_{34}\text{H}_{34}\text{N}_4\text{O}_8 \cdot 4\text{H}_2\text{O}$ ) Co, C, H, N, amine: calcd, 42.81; found, 40.0.

**Bis(pyridoxylidene-2(S)-phenylalaninato)nickel Hydrate.** Ni(HPL-2(S)-phe)<sub>2</sub>·3.5H<sub>2</sub>O was prepared in the same way as the corresponding valine complex and isolated as a brown crystalline material. Anal. ( $\text{NiC}_{34}\text{H}_{34}\text{N}_4\text{O}_8 \cdot 3.5\text{H}_2\text{O}$ ) Ni, C, H, N.

**Pyridoxylidene-2(S)-phenylalaninatocopper(II) Hexahydrate.** CuPL-2(S)-phe·6H<sub>2</sub>O was prepared as the previous copper complexes except that CuSO<sub>4</sub>·5H<sub>2</sub>O was used. A green powder was isolated. Anal. ( $\text{CuC}_{17}\text{H}_{16}\text{N}_2\text{O}_4 \cdot 6\text{H}_2\text{O}$ ) Cu, N; C: calcd, 47.39; found, 46.50; H: calcd, 5.38; found, 4.03.<sup>43</sup> A second preparation gave similar results. Anal. ( $\text{CuC}_{17}\text{H}_{16}\text{N}_2\text{O}_4 \cdot 6\text{H}_2\text{O}$ ) Cu, N; C: calcd, 47.39; found, 47.89; H: calcd, 5.38; found, 4.24.

**Bis(pyridoxylidene-2(S)-tryptophanato)manganese(II) Hemihydrate.** Yellow-brown Mn(HPL-2(S)-trp)<sub>2</sub>·0.5H<sub>2</sub>O was prepared in the same manner as the corresponding alanine complex except that methanol was the solvent. Anal. ( $\text{MnC}_{38}\text{H}_{36}\text{N}_6\text{O}_8 \cdot 0.5\text{H}_2\text{O}$ ) Mn, C, H, N.

**Bis(pyridoxylidene-2(S)-tryptophanato)iron(II) Dihydrate.** Fe(HPL-2(S)-trp)<sub>2</sub>·2H<sub>2</sub>O was prepared in the same manner as the preceding iron(II) complexes. The green solution resulting from the synthesis was introduced onto a silica gel column and developed with methanol. A green band spread down into the column and a reddish zone developed at the top. The material at the top of the column was taken to be oxidized compound. The green band was eluted from the column with methanol. The solvent was removed by evaporation and the green crystalline product dried at room temperature in vacuo. Anal. ( $\text{FeC}_{38}\text{H}_{36}\text{N}_6\text{O}_8 \cdot 2\text{H}_2\text{O}$ ) Fe, C, H, N.

**Bis(pyridoxylidene-2(S)-tryptophanato)cobalt(II) Octahydrate.** Co(HPL-2(S)-trp)<sub>2</sub>·8H<sub>2</sub>O was prepared in the same way as the Co(II) complexes above. Anal. ( $\text{CoC}_{38}\text{H}_{36}\text{N}_6\text{O}_8 \cdot 8\text{H}_2\text{O}$ ) Co, C, H, N, amine.

**Bis(pyridoxylidene-2(S)-tryptophanato)nickel(II) Octahydrate.** Ni(HPL-2(S)-trp)<sub>2</sub>·8H<sub>2</sub>O was prepared as follows. A solution of 2.034 g of H<sub>2</sub>PL-HCl (10 mmol) was dissolved in 25 mL of methanol by the addition of 15 mL of 0.156 N aqueous NaOH (10 mmol). A second solution of 2.04 g of trp (10 mmol) was prepared by adding tryptophan to a methanolic solution of 15 mL of 0.156 N aqueous NaOH (10 mmol). The first solution was then slowly added to the second. After the appearance of an orange-yellow solution, 1.19 g of NiCl<sub>2</sub>·6H<sub>2</sub>O (5 mmol) was added as a solid. After stirring at room temperature for 1 h, the solution was cooled to 0 °C. A brown-yellow precipitate that formed after 12 h was filtered, washed first with methanol, and then with diethyl ether, and then dried at room temperature in vacuo for several hours. Anal. ( $\text{NiC}_{38}\text{H}_{36}\text{N}_6\text{O}_8 \cdot 8\text{H}_2\text{O}$ ) Ni, C, H, N.

**Pyridoxylidene-2(S)-tryptophanato-copper(II) Tetrahydrate.** CuPL-2(S)-trp·4H<sub>2</sub>O was prepared in the same way as the preceding copper complexes. Anal. ( $\text{CuC}_{19}\text{H}_{17}\text{N}_3\text{O}_4 \cdot 4\text{H}_2\text{O}$ ) Cu, C, N; H: calcd, 5.11; found, 4.46.

## Results and Discussion

The Mn(II), Co(II), Ni(II), and Cu(II) complexes prepared above (with the one noted exception) are stable at room temperature if kept tightly sealed and stored in a desiccator. Because the Fe(II) compounds are very air sensitive they must be stored under an inert atmosphere and used within a few days of their preparation. All of the compounds are slightly soluble in warm water or methanol but decompose in aqueous solutions of pH < 4 or pH > 9.

**X-Ray Diffraction Data.** The x-ray diffraction data for powdered samples of the complexes prepared above are given in Table II.<sup>42</sup> The standard deviation for the tabulated *d* spacings is ca. 0.13 Å. The similarity of powder patterns indicates that the following sets of complexes are x-ray isomorphous: Co(HPLgly)<sub>2</sub>·4H<sub>2</sub>O and Ni(HPLgly)<sub>2</sub>·4H<sub>2</sub>O; Mn(HPL-2(S)-ala)<sub>2</sub>·H<sub>2</sub>O, Co(HPL-2(S)-ala)<sub>2</sub>·4H<sub>2</sub>O, and Ni(HPL-2(S)-ala)<sub>2</sub>·4H<sub>2</sub>O; Mn(HPL-2(S)-val)<sub>2</sub>·2H<sub>2</sub>O, Fe(HPL-DL-val)<sub>2</sub>·H<sub>2</sub>O, Co(HPL-2(S)-val)<sub>2</sub>·4H<sub>2</sub>O, and Ni(HPL-2(S)-val)<sub>2</sub>·3.5H<sub>2</sub>O; Co(HPL-2(S)-phe)<sub>2</sub>·4H<sub>2</sub>O and Ni(HPL-2(S)-phe)<sub>2</sub>·3.5H<sub>2</sub>O; and Mn(HPL-2(S)-trp)<sub>2</sub>·0.5H<sub>2</sub>O, Co(HPL-2(S)-trp)<sub>2</sub>·8H<sub>2</sub>O, and Ni(HPL-2(S)-trp)<sub>2</sub>·8H<sub>2</sub>O. Although the Cu complexes as a group show

Table IIIA. Magnetic Susceptibility Data

Compd	$\chi_M^c$ , cgsu	T, K	$\chi_M'$ , cgsu	$\mu_{\text{eff}}$ , $\mu_B$
CuPLgly $\cdot$ 2H <sub>2</sub> O	-101	290.1	1 692	1.96
		102.0	4 092	1.85
CuPL-2(S)-ala $\cdot$ 2H <sub>2</sub> O	-113	297.7	1 635	1.97
		78.0	5 153	1.79
CuPL-2(S)-val	-111	297.6	1 621	1.98
		103.0	4 110	1.85
CuPL-2(S)-phe $\cdot$ 6H <sub>2</sub> O	-230	289.8	1 661	1.96
		102.9	4 097	1.84
CuPL-2(S)-trp $\cdot$ 4H <sub>2</sub> O	-212	286.8	1 684	1.97
		78.0	5 100	1.78
Ni(HPLgly) <sub>2</sub> $\cdot$ 4H <sub>2</sub> O	-241	301.2	3 800	3.04
		78.0	14 280	2.99
Ni(HPL-2(S)-ala) <sub>2</sub> $\cdot$ 4H <sub>2</sub> O	-253	298.8	3 901	3.04
		78.0	14 540	3.00
Ni(HPL-2(S)-val) <sub>2</sub> $\cdot$ 3.5H <sub>2</sub> O	-271	299.3	4 110	3.14
		105.3	11 020	3.04
Ni(HPL-2(S)-phe) <sub>2</sub> $\cdot$ 3.5H <sub>2</sub> O	-297	298.3	3 911	3.06
		109.5	10 150	2.98
Ni(HPL-2(S)-trp) <sub>2</sub> $\cdot$ 8H <sub>2</sub> O	-323	297.6	3 990	3.23
		125.8	10 440	3.23
Co(HPLgly) <sub>2</sub> $\cdot$ 4H <sub>2</sub> O	-241	296.4	8 969	4.61
		78.0	33 110	4.54
Co(HPL-2(S)-ala) <sub>2</sub> $\cdot$ 4H <sub>2</sub> O	-253	289.8	9 083	4.59
		106.3	23 920	4.51
Co(HPL-2(S)-val) <sub>2</sub> $\cdot$ 4H <sub>2</sub> O	-279	296.6	9 070	4.64
		109.5	23 260	4.51
Co(HPL-2(S)-phe) <sub>2</sub> $\cdot$ 4H <sub>2</sub> O	-304	297.0	7 677	4.27
		78.0	27 350	4.10
Co(HPL-2(S)-trp) <sub>2</sub> $\cdot$ 8H <sub>2</sub> O	-330	296.6	7 691	4.27
		109.3	19 740	4.15
Fe(HPLgly) <sub>2</sub>	-199	296.0	10 040	4.88
		78.0	36 780	4.79
Fe(HPL-DL-ala) <sub>2</sub> $\cdot$ 10H <sub>2</sub> O	-331	298.9	9 980	4.88
		78.0	37 850	4.86
Fe(HPL-DL-val) <sub>2</sub> $\cdot$ 2H <sub>2</sub> O	-243	301.2	9 980	4.91
		78.0	36 700	4.79
Fe(HPL-2(S)-phe) <sub>2</sub> $\cdot$ 15H <sub>2</sub> O	-430	298.2	10 020	4.93
		78.0	36 630	4.78
Fe(HPL-2(S)-trp) <sub>2</sub> $\cdot$ 2H <sub>2</sub> O	-252	296.5	10 200	4.92
		78.0	36 460	4.77
Mn(HPL-2(S)-ala) <sub>2</sub> $\cdot$ H <sub>2</sub> O	-215	296.4	14 750	5.91
		78.0	55 800	5.90
Mn(HPL-2(S)-val) <sub>2</sub> $\cdot$ 2H <sub>2</sub> O	-245	294.3	14 900	5.92
		78.0	55 800	5.90
Mn(HPL-2(S)-trp) <sub>2</sub> $\cdot$ 0.5H <sub>2</sub> O	-241	299.6	14 700	5.93
		78.0	56 200	5.92

certain similarities in their powder patterns, they are apparently not isomorphous to any of the sets of compounds mentioned above. The fact that Fe(HPLgly)<sub>2</sub>, Fe(HPL-DL-ala)<sub>2</sub> $\cdot$ 10H<sub>2</sub>O, and Fe(HPL-2(S)-phe)<sub>2</sub> $\cdot$ 15H<sub>2</sub>O do not fit into the above series of isostructural compounds does not necessarily imply that these three compounds are different than their Mn, Ni, or Co analogues. It is likely that the large differences in lattice water between, say, Co(HPL-2(S)-phe)<sub>2</sub> $\cdot$ 4H<sub>2</sub>O and Fe(HPL-2(S)-phe)<sub>2</sub> $\cdot$ 15H<sub>2</sub>O has caused a change in unit cell parameters which affects the powder pattern of the latter compound in a way that is not obviously seen in the *d* spacings. It is, however, likely that the copper complexes are structurally different than their Mn, Fe, Co, and Ni analogues. This assertion is further supported by the elemental analyses which clearly classify the Mn, Fe, Co, and Ni compounds as bis complexes and the Cu compounds as mono complexes.

**Magnetic Susceptibility Data.** A summary of the magnetic susceptibilities at 78 K and room temperature is presented in Table IIIA. The experimental magnetic susceptibilities and moments as a function of temperature for the complexes are listed in Table IIIB.<sup>42</sup> The estimated uncertainty in  $\mu_{\text{eff}}$  is  $\pm 0.03 \mu_B$ . A plot of  $1/\chi_M'$  vs. *T* for each of the complexes was linear within experimental uncertainty over the temperature range studied. Values of  $\theta$ , the Weiss constant, were

taken from these plots and fall in the range -26 to -19 K for the copper complexes, -1 to -10 K for the nickel complexes, ca. -6 K for the cobalt complexes, and ca. -6 K for the iron complexes (Table IIIB). The copper complexes have room temperature moments of ca.  $1.96 \mu_B$  which fall to ca.  $1.80 \mu_B$  at liquid nitrogen temperature. The value of  $\mu_{\text{eff}}$  clearly indicates one unpaired electron as expected for monomeric divalent copper complexes. The decrease of  $\mu_{\text{eff}}$  with decreasing temperature and the slightly higher than spin-only value of the room temperature moment implies the presence of a low-lying excited term which at high temperature is able to mix some of its orbital angular momentum with the spin angular momentum of the ground term via spin-orbit coupling.<sup>44,45</sup> This mixing is quite common for Cu(II) complexes with distorted ligand fields.<sup>46</sup> The low-symmetry component of the ligand field also serves to split the ground term. Unfortunately, the magnetic data displayed by these copper complexes do not uniquely describe the coordination sphere. Thus, five- or six-coordinate Cu(II) complexes both show the same susceptibility vs. temperature behavior.<sup>46</sup> It is therefore not possible to decide on the coordination geometry of the Cu(II) complexes solely on the basis of  $\mu_{\text{eff}}$ .

The nickel complexes have room temperature moments of ca.  $3.23$  to  $3.04 \mu_B$  which fall to ca. 95% of this value at 100 K. These values of  $\mu_{\text{eff}}$  are slightly higher than the spin-only value of  $2.83 \mu_B$  expected for two unpaired electrons and are very characteristic of the magnetic properties of distorted octahedral nickel(II) complexes.<sup>44,45</sup> Because the plots of  $1/\chi_M'$  vs. temperature are linear from 78 to 300 K, no temperature-independent paramagnetism correction was included in the calculation of  $\mu_{\text{eff}}$ .

The cobalt complexes have room temperature moments which may be divided into two classes. The three complexes with aliphatic side chains have  $\mu_{\text{eff}}$  of ca.  $4.6 \mu_B$  while the two complexes with aromatic side chains have  $\mu_{\text{eff}}$  ca.  $4.3 \mu_B$ . These moments are higher than the spin-only value of  $3.87 \mu_B$  expected for three unpaired electrons but lower than the value of  $5 \mu_B$  which is usually observed for regular octahedral Co(II) complexes. The mechanism which best accounts for the lower values of  $\mu_{\text{eff}}$  involves a partial quenching of the orbital angular momentum by a low-symmetry ligand field component. The fact that the more bulky side chains of phe and trp cause a greater reduction in  $\mu_{\text{eff}}$  relative to the gly, ala, and val side chains is consistent with this mechanism. No temperature-independent paramagnetism correction was included in the calculation of  $\mu_{\text{eff}}$ . As for other distorted octahedral cobalt(II) complexes with low symmetry split orbital triplet ground terms, the values of  $\mu_{\text{eff}}$  decrease to ca. 95% of their room temperature value at 100 K.

The magnetic susceptibility data for the iron complexes (Table IIIB) are also characteristic of distorted octahedral iron(II) coordination. The room temperature value for  $\mu_{\text{eff}}$  of  $4.90 \mu_B$  is exactly equal to the spin-only value expected for four unpaired electrons. Even though the majority of octahedral Fe(II) complexes have  $\mu_{\text{eff}}$  in excess of  $5.2 \mu_B$ , it is possible for a low-symmetry ligand field component to completely remove the orbital angular momentum contribution. The very small temperature dependence (ca. 3% or less) indicates that the ground term has been split to the extent of  $1000 \text{ cm}^{-1}$  or more.<sup>47</sup>

The temperature-independent values of  $\mu_{\text{eff}}$  for the manganese complexes of ca.  $5.92 \mu_B$  are exactly that expected for five unpaired electrons. This is consistent with the  ${}^6A_{1g}$  ground term of octahedral Mn(II). Although it is possible that other stereochemistries of Mn(II) could display such magnetic behavior, the propensity of Mn(II) to form six-coordinate octahedral complexes would appear to rule out this possibility.

Table IV. Mössbauer Effect Data

Compd	T, K	$\Delta E_Q$ , mm/s	$\delta$ , <sup>a</sup> mm/s	$\Gamma_1$ , <sup>b</sup> mm/s	$\Gamma_2$ , <sup>b</sup> mm/s	Rel % effect
Fe(HPLgly) <sub>2</sub>	78	2.86 (2)	1.160 (7)	0.50 (3)	0.52 (3)	12
	300	2.30 (2)	0.992 (8)	0.59 (4)	0.62 (5)	1
Fe(HPL-2(S)-ala) <sub>2</sub> ·10H <sub>2</sub> O	78	2.90 (3)	1.157 (8)	0.62 (4)	0.68 (5)	15
	300	2.30 (3)	0.974 (9)	0.61 (5)	0.63 (5)	2
Fe(HPL-2(S)-val) <sub>2</sub> ·2H <sub>2</sub> O	78	2.88 (1)	1.152 (4)	0.48 (3)	0.48 (3)	10
	300	2.26 (2)	0.979 (5)	0.52 (4)	0.54 (4)	2
Fe(HPL-2(S)-phe) <sub>2</sub> ·15H <sub>2</sub> O	78	2.88 (2)	1.191 (7)	0.47 (3)	0.58 (3)	15
	300	2.25 (2)	0.988 (4)	0.54 (4)	0.63 (5)	2
Fe(HPL-2(S)-trp) <sub>2</sub> ·2H <sub>2</sub> O	78	2.86 (2)	1.110 (7)	0.38 (4)	0.32 (4)	10
	300	2.29 (2)	0.971 (6)	0.45 (5)	0.48 (5)	3

<sup>a</sup> Relative to natural iron foil. <sup>b</sup> Full-width at half-maximum.

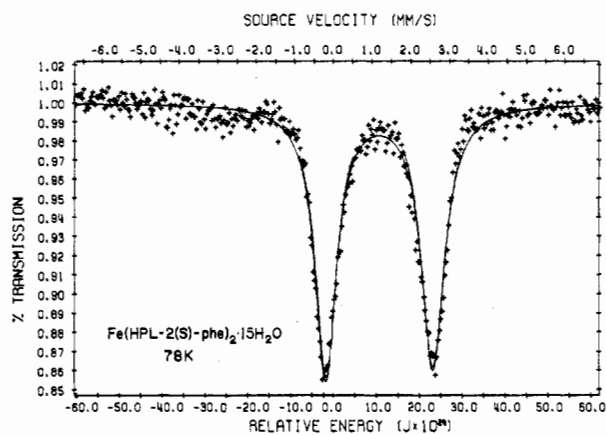


Figure 1. The Mössbauer spectrum of Fe(HPL-2(S)-phe)<sub>2</sub>·15H<sub>2</sub>O at 78 K.

**Mössbauer Effect Data.** The iron(II) complexes of the pyridoxylideneamino acids show Mössbauer effect spectra which are consistent with high-spin distorted octahedral Fe(II). The 78 K spectrum of Fe(HPL-2(S)-phe)<sub>2</sub>·15H<sub>2</sub>O is representative of the group and is shown in Figure 1. The appropriate Mössbauer spectral parameters for all the Fe(II) complexes are given in Table IV. Both the quadrupole splitting,  $\Delta E_Q$ , and the chemical isomer shift,  $\delta$ , decrease with increasing temperature. The former parameter increases from ca. 2.27 mm/s at 300 K to ca. 2.86 mm/s at 78 K. This behavior is typical of distorted octahedral iron(II) complexes.<sup>49</sup> The parameter  $\delta$  increases from ca. 0.98 mm/s to ca. 1.15 mm/s in this same temperature range. Such an increase in  $\delta$  may be attributable to, at least in part, a second-order Doppler shift arising from lattice effects. Because our experiments at 78 K were done with the source at room temperature it is possible that the absorber lattice changed considerably relative to the source lattice. Such changes could conceivably account for changes in  $\delta$  up to ca. 15% of its room temperature value.<sup>50</sup> Whereas this second-order Doppler effect does not allow us to compare the increase in  $\delta$  as a function of temperature it is possible to arrange the series of Fe(II) complexes in order of increasing  $\delta$ . If we consider the 78 K  $\delta$  values given in Table IV the following order emerges: phe (1.19) > gly (1.16) ~ ala (1.16) ~ val (1.15) > trp (1.11). This series parallels an increase in the  $pK_a$  of the amino acid carboxyl group; phe ( $pK_a = 1.83$ ) > gly, ala, val ( $pK_a = 2.33$ ) > trp ( $pK_a = 2.38$ ). This correlation is to be expected because a stronger base would tend to form structure 14 in preference

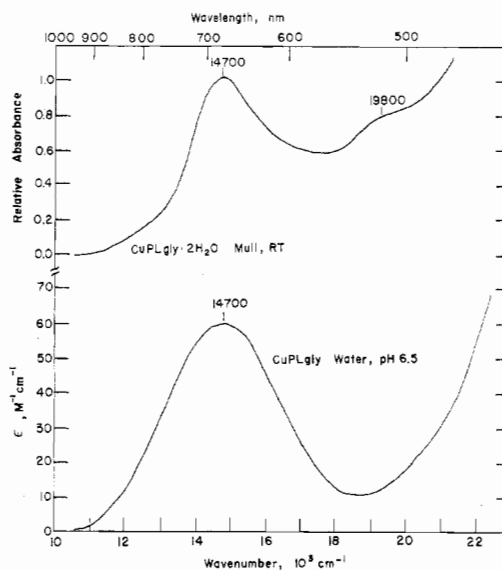
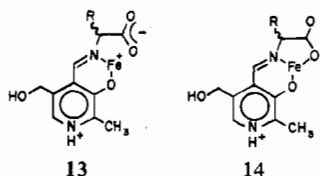


Figure 2. The visible spectrum of CuPLgly·2H<sub>2</sub>O.

to 13 thereby increasing  $\delta$ . It is interesting to note that the magnitude of the temperature dependence of  $\delta$  for each compound also follows this series. Table IV also contains percent effect data for each of the complexes. These values increase from ca. 1% at room temperature to ca. 10% at 78 K. Such a high temperature dependence is normally associated with a low Debye temperature for the solid. This low Debye temperature is indicative of rather weak ligand binding of the Fe(II). The values of the line widths given in Table IV are slightly broader than the line widths of other high-spin octahedral Fe(II) complexes. The breadth of the lines may be ascribed to slightly different bonding configurations at different iron sites within the crystal. These slightly different configurations may be associated with a nonuniform distribution of the lattice water of hydration throughout the crystal.

**Electronic Spectra of the Cu(II) Complexes.** The visible spectrum of CuPLgly·2H<sub>2</sub>O shown in Figure 2 is typical of the visible absorption spectra of all the (pyridoxylideneamino acid)copper(II) complexes. Both the room temperature mull spectrum and the solution spectrum obtained at a pH of 6.5 have a low-intensity symmetric band at ca. 14700 cm<sup>-1</sup> which may be assigned to the ligand field transition commonly observed for Cu(II) complexes. This band is broader in solution than in the solid state. An additional low-intensity band appears at ca. 19800 cm<sup>-1</sup> in the mull spectrum of CuPLgly·2H<sub>2</sub>O (see Figure 2). This spectral feature is common to all the Cu complexes. It also appears in the aqueous solution spectrum of pyridoxal and therefore is likely an intraligand absorption band. The ligand field and intraligand absorption bands observed for each of the copper complexes are presented in Table V. In aqueous solution at a pH of 6.5 and in the solid state the position of the ligand field transition remains

Table V. Electronic Absorption Bands for the Cu(II) Complexes

Compd	Solvent or Matrix	Temp, K, or pH	Ligand field <sup>a</sup>	Intraligand <sup>a</sup> $\tilde{\nu}_{\max}$ , cm <sup>-1</sup> × 10 <sup>3</sup>
			$\tilde{\nu}_{\max}$ , cm <sup>-1</sup> × 10 <sup>3</sup>	
CuPLgly·2H <sub>2</sub> O	H <sub>2</sub> O	pH 6.5	14.70 (60)	26.3 (6500), 27.4 (6700), 44.4 (20700)
	Mull	Amb	14.70	19.8, 26.2, 27.4, 44.4
CuPL-DL-ala·2H <sub>2</sub> O	H <sub>2</sub> O	pH 6.5	14.82 (100)	19.8 (30), 25.5 (6000), 26.2 (6000), 36.3 (6000), 44.5 (18500)
	Mull	Amb	15.00	19.8, 25.8, 36.3
	Mull	23	15.00	
CuPL-2(S)-val	H <sub>2</sub> O	pH 6.5	14.60 (114)	19.8 (35), 26.6 (6335), 44.4 (20000)
	Mull	Amb	14.60	19.8, 26.6
	H <sub>2</sub> O	pH 3.2	14.64 (70)	
CuPL-2(S)-phe·6H <sub>2</sub> O	H <sub>2</sub> O	pH 6.5	14.60 (75)	25.5 (4640), 26.2 (4625), 35.35 (4300), 44.4 (11800), 46.5 (13500)
	H <sub>2</sub> O	pH 8.3	15.75 (110)	
	CH <sub>3</sub> OH	Neutral	13.50 (35)	
	Mull	Amb	14.65	19.4, 26.0, 35.3
	Mull	Amb	14.60 (80)	19.8 (40), 22.7 (4100), 25.0 (4325)
CuPL-2(S)-trp·4H <sub>2</sub> O	H <sub>2</sub> O	pH 6.5	14.60 (80)	19.8, 22.7, 25.0
	Mull	Amb	14.60	

<sup>a</sup> Apparent molar absorptivity at the band maximum given in parentheses. <sup>b</sup>  $e^{\text{app}}$ , mol<sup>-1</sup> L<sup>-1</sup> cm<sup>-1</sup>; see ref 35.

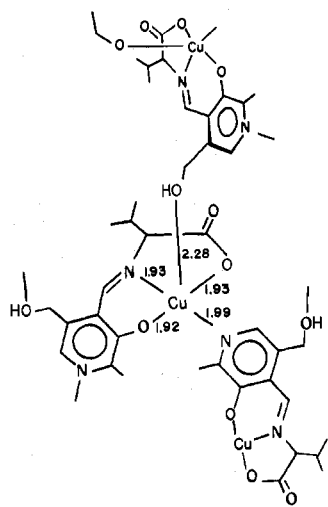
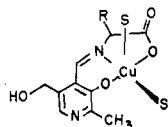


Figure 3. A portion of the crystal structure of CuPL-DL-val.<sup>30</sup>

nearly constant at 14 700 cm<sup>-1</sup>. In contrast, this band is lowered by ca. 1000 cm<sup>-1</sup> when CuPL-2(S)-phe·6H<sub>2</sub>O is dissolved in methanol. This shift is consistent with the weaker ligand methanol replacing water in solvent-occupied coordination positions. The solid-state structure of CuPL-DL-val determined by Cutfield et al.<sup>30</sup> is shown in Figure 3. Because of the similarity of the solid and the solution phase ligand field spectrum it seems likely that the solid-state and the solution structure of CuPL-DL-val are similar. Such a situation is illustrated in **15** where S indicates a solvent molecule.



15

The additional copper coordination sites are occupied in the solid state by the pyridine nitrogen and 5'-hydroxymethyl oxygen of adjacent molecules thereby yielding a weakly bonded polymer.<sup>30</sup> Apparently because of solvation the average ligand field present in solution is the same as in the solid state resulting in essentially identical ligand field spectra. The more flexible coordination sphere in the solvated molecule (**15**) may account for the broadness of the solution-phase band relative to the solid-state band. As indicated in Table V, this ligand field band in CuPL-2(S)-ala·2H<sub>2</sub>O in a KBr matrix has been shifted to 12 900 cm<sup>-1</sup>. Similar shifts are observed in the KBr

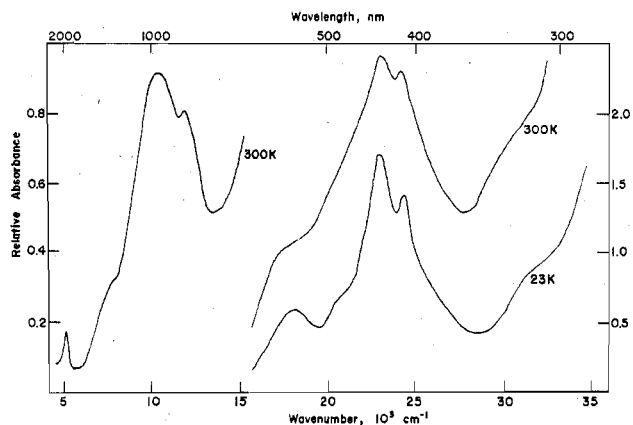


Figure 4. The electronic spectrum of Ni(HPL-2(S)-val)<sub>2</sub>·3.5H<sub>2</sub>O.

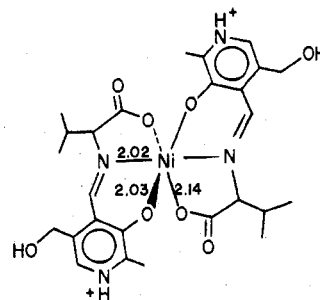


Figure 5. A portion of the structure of Ni(HPL-DL-val)<sub>2</sub>·7.4H<sub>2</sub>O.<sup>31</sup>

spectra of the copper PLtrp and the copper PLval complexes. The PLphe and PLgly copper complexes are apparently decomposed at the relatively high concentrations needed to obtain the ligand field spectra. This shift to lower energy indicates that the coordination geometry has been altered in going from the pure solid-phase complex to the KBr matrix. This change most likely results from the disruption of the pyridine nitrogen and 5'-hydroxymethyl oxygen bridging polymeric network in the KBr matrix.

In addition to the 19 800-cm<sup>-1</sup> band mentioned above three additional absorptions are observed in the 20 000–40 000-cm<sup>-1</sup> region of the spectrum (see Table V). The intensity of these bands ( $\epsilon \approx 6000$  and 20 000 cm<sup>-1</sup> M<sup>-1</sup>) indicate that they result from intraligand electronic transitions. These particular bands have been assigned as such for the similar salicylidene compounds<sup>51,52</sup> and we shall not consider them further.

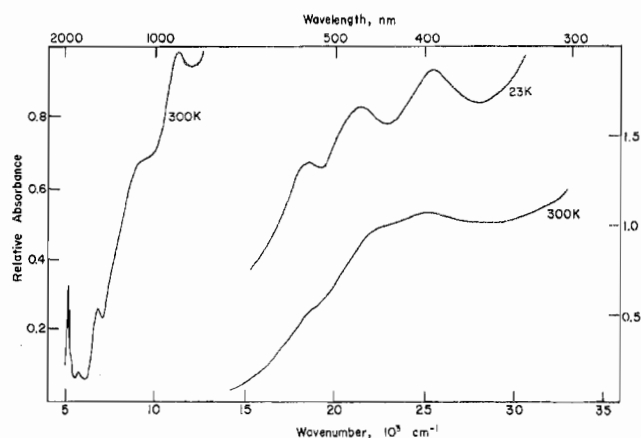
**Electronic Spectra of the Ni(II) Complexes.** The electronic absorption spectrum of Ni(HPL-2(S)-val)<sub>2</sub>·3.5H<sub>2</sub>O is shown

Table VI. Electronic Absorption Bands in the Nickel Complexes<sup>a</sup>

Compd	$\tilde{\nu}_{\max}$ , $\text{cm}^{-1} \times 10^3$	Assignment
Ni(HPLgly) <sub>2</sub> ·4H <sub>2</sub> O <i>Dq</i> = 1080 $\beta^b$ = 0.54	5.20, 7.00	Water bands
	10.00 sh, 11.50	$\nu_1$ : ${}^3A_{2g}(F) \rightarrow {}^3T_{2g}(F)$
	16.30 sh, 17.00 sh	$\nu_2$ : ${}^3A_{2g}(F) \rightarrow {}^3T_{1g}(F)$
	19.5 sh, 25.4	Intraligand bands
	29.3	
Ni(HPL-2(S)-ala) <sub>2</sub> ·4H <sub>2</sub> O <i>Dq</i> = 940 $\beta$ = 0.65	23.10	$\nu_3$ : ${}^3A_{2g}(F) \rightarrow {}^3T_{1g}(P)$
	5.20	Water bands
	8.7 sh, 10.00	$\nu_1$ : ${}^3A_{2g}(F) \rightarrow {}^3T_{2g}(F)$
	14.2 sh, 15.4 sh	$\nu_2$ : ${}^3A_{2g}(F) \rightarrow {}^3T_{1g}(F)$
	23.8 sh	$\nu_3$ : ${}^3A_{2g}(F) \rightarrow {}^3T_{1g}(P)$
Ni(HPL-2(S)-val) <sub>2</sub> ·3.5H <sub>2</sub> O <i>Dq</i> = 1090	27.0	Intraligand band
	5.20, 7.10	Water bands
	5.90	Ligand overtone
	10.30, 11.90	$\nu_1$ : ${}^3A_{2g}(F) \rightarrow {}^3T_{2g}(F)$
	17.40	$\nu_2$ : ${}^3A_{2g}(F) \rightarrow {}^3T_{1g}(F)$
Ni(HPL-2(S)-phe) <sub>2</sub> ·3.5H <sub>2</sub> O	23.0, 24.3	Intraligand bands
	7.2 sh	Water bands
	10.0 sh, 11.10, 12.4 sh	$\nu_1$ : ${}^3A_{2g}(F) \rightarrow {}^3T_{2g}(F)$
	23.25, 24.40, 26.32, 41.70	$\nu_3$ + intraligand
	5.2, 7.20	Water bands
Ni(HPL-2(S)-trp) <sub>2</sub> ·8H <sub>2</sub> O	10.50, 11.25 sh	$\nu_1$ : ${}^3A_{2g}(F) \rightarrow {}^3T_{2g}(F)$
	15.0 sh	$\nu_2$ : ${}^3A_{2g}(F) \rightarrow {}^3T_{1g}(F)$
	24.9	Intraligand band

<sup>a</sup> Room temperature mull spectra. Abbreviation: sh = shoulder. <sup>b</sup>  $B_0 = 1084 \text{ cm}^{-1}$ .

in Figure 4 and Table VI contains the absorption bands found in the 5000–35 000- $\text{cm}^{-1}$  region for all the Ni(II) complexes. These spectra may be interpreted by reference to the crystal structure of Ni(HPL-DL-val)<sub>2</sub>·7.4H<sub>2</sub>O as determined by Capasso et al.<sup>31</sup> and illustrated in Figure 5. In this compound the nickel ion is surrounded by a distorted octahedral array of ligand atoms. This array should give rise to three sets of low-intensity absorption bands at ca. 10 000, 15 000, and 20 000  $\text{cm}^{-1}$  in analogy with other octahedral Ni(II) complexes.<sup>53</sup> The lowest energy  ${}^3A_{2g}(F) \rightarrow {}^3T_{2g}(F)$  transition is clearly observed in our nickel complexes as a structured band centered at ca. 10 000  $\text{cm}^{-1}$ . The presence of a very intense intraligand electronic absorption band extending into the visible obscures the weak transitions  $\nu_2$  and  $\nu_3$  to the  ${}^3A_{2g}$  and  ${}^3T_{1g}(P)$  ligand field states, respectively. The former transition,  $\nu_2$ , is visible in Ni(HPLgly)<sub>2</sub>·4H<sub>2</sub>O, Ni(HPL-2(S)-ala)<sub>2</sub>·4H<sub>2</sub>O, Ni(HPL-2(S)-val)<sub>2</sub>·3.5H<sub>2</sub>O, and Ni(HPL-2(S)-trp)<sub>2</sub>·8H<sub>2</sub>O as a shoulder at ca. 15 000  $\text{cm}^{-1}$ . The  $\nu_3$  band is tentatively assigned in Table VI for the gly and the ala compounds. By using these assignments, values for the crystal field parameters *Dq*, *B*, and  $\beta$  were calculated with the expressions of König.<sup>54,55</sup> These results are also presented in Table VI. The five *Dq* values obtained from the  ${}^3A_{2g}(F) \rightarrow {}^3T_{2g}(F)$  transition are

Figure 6. The electronic spectrum of Co(HPL-2(S)-phe)<sub>2</sub>·4H<sub>2</sub>O.

typical of distorted octahedral Ni(II).<sup>53</sup> The values of  $\beta$ , however, are uncertain because of the difficulty in assigning the exact position of  $\nu_2$  and  $\nu_3$ .

**Electronic Spectra of the Cobalt(II) Complexes.** Because the Co(II) complexes are isostructural with their Ni(II) analogues, ligand field spectra typical of distorted octahedral Co(II) are expected. The mull electronic spectrum of Co(HPL-2(S)-phe)<sub>2</sub>·4H<sub>2</sub>O at room temperature and 23 K is presented in Figure 6. Very similar spectra are obtained for the remaining Co(II) complexes as indicated by the numerical results presented in Table VII. Three ligand field transitions are observed in addition to the intense intraligand bands. The lowest energy ligand field band near 9000  $\text{cm}^{-1}$  is assigned to  $\nu_1$ , the  ${}^4T_{1g}(F) \rightarrow {}^4T_{2g}(F)$  transition. The band near 19 000  $\text{cm}^{-1}$  is assigned to  $\nu_2$ , the  ${}^4T_{1g}(F) \rightarrow {}^4A_{2g}(F)$  transition, and the band near 22 000  $\text{cm}^{-1}$  is assigned to  $\nu_3$ , the  ${}^4T_{1g}(F) \rightarrow {}^4T_{1g}(P)$  transition. In addition to the water overtone at ca. 7200  $\text{cm}^{-1}$  a very weak band is visible near 8000  $\text{cm}^{-1}$  which disappears upon cooling. We have assigned this band to the spin-forbidden  ${}^4T_{1g}(F) \rightarrow {}^2E_g(G)$  transition.<sup>56</sup> The spectra of Co(HPL-2(S)-phe)<sub>2</sub>·4H<sub>2</sub>O and Co(HPL-2(S)-trp)<sub>2</sub>·8H<sub>2</sub>O show significant splitting of the  $\nu_1$  band. This splitting may result from the greater steric requirements of the phe and trp side chains relative to gly, ala, and val. The greater bulk of the side chains apparently causes a pronounced reduction in the ligand field symmetry.

The greater wealth of spectral data obtained for the cobalt complexes as compared to the nickel complexes permits the calculation of a more extensive set of ligand field parameters. A least-squares fit of these experimental band positions to the electrostatic matrix elements of McClure<sup>57</sup> gives the parameters and calculated values of  $\nu_1$ ,  $\nu_2$ , and  $\nu_3$  shown in Table

Table VII. Ligand-Field Bands and Derived Parameters for the Co(II) Complexes<sup>a</sup>

Parameter	Co(HPLgly) <sub>2</sub> ·4H <sub>2</sub> O	Co(HPLala) <sub>2</sub> ·4H <sub>2</sub> O	Co(HPLval) <sub>2</sub> ·4H <sub>2</sub> O	Co(HPLphe) <sub>2</sub> ·4H <sub>2</sub> O	Co(HPLtrp) <sub>2</sub> ·8H <sub>2</sub> O
$\nu_1$ (300 K)	8510	8900	8710	8700, 11700	10750, 13500
(23 K)	8500	8900	8700	8700, 12150	10800, 13500
$\nu_2$ (300 K)	19230	17900	17000	19050	17540
(23 K)	19200	17900	17000	19050	17540
$\nu_3$ (300 K)	22200	22200		21300	22730
(23 K)	22150	22250	22200	21300	22900
$\nu_{sf}^b$ (300 K)	8900	7020	7500	7700	7700
(23 K)		7000			
<i>Dq</i>	1025	1010	997	1014	939
<i>B</i>	966	868	1000	908	1057
<i>C</i>	4280	4180	4290	4400	4518
$\beta$	0.87	0.78	0.90	0.81	0.95
$\nu_1^{\text{calcd}}$	8990 (+6) <sup>c</sup>	8900 (+0)	8710 (+0)	8910 (-13)	8150 (-33)
$\nu_2^{\text{calcd}}$	19240 (+0)	19000 (+6)	18680 (+10)	19050 (+0)	17540 (+0)
$\nu_3^{\text{calcd}}$	22210 (+0)	20720 (-7)	22450 (+1)	21310 (+0)	22760 (+0)

<sup>a</sup> All values, except  $\beta$ , in  $\text{cm}^{-1}$ . <sup>b</sup>  $\nu_{sf} = {}^4T_{1g}(F) \rightarrow {}^2E_g(G)$ . <sup>c</sup> Values in parentheses are percent deviation from the experimental values.

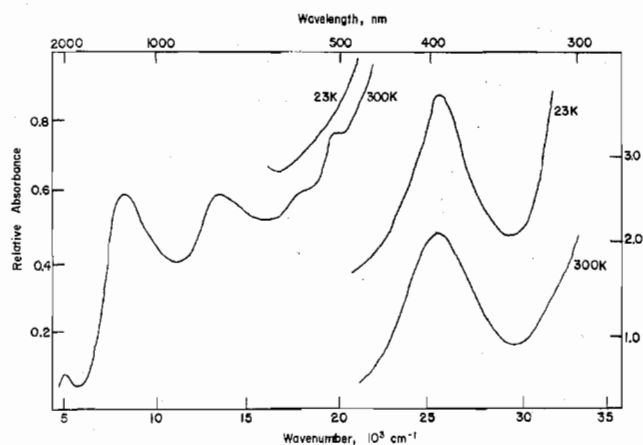


Figure 7. The electronic spectrum of Fe(HPL-2(S)-val)<sub>2</sub>·2H<sub>2</sub>O.

Table VIII. Fe(II) Ligand Field Bands<sup>a</sup>

Compd	<sup>5</sup> T <sub>2g</sub> → <sup>5</sup> E <sub>g</sub> , cm <sup>-1</sup> × 10 <sup>3</sup>	Spin- forbidden bands	Dq, cm <sup>-1</sup>
Fe(HPLgly) <sub>2</sub>	8.50, 14.00	17.20, 19.80	1125
Fe(HPL-DL-ala) <sub>2</sub> ·10H <sub>2</sub> O	8.50, 14.10	16.90	1130
Fe(HPL-DL-val) <sub>2</sub> ·2H <sub>2</sub> O	8.40, 14.20	17.25, 18.80	1130
Fe(HPL-2(S)-phe) <sub>2</sub> ·15H <sub>2</sub> O	9.85, 14.00	17.30, 19.00	1190
Fe(HPL-2(S)-trp) <sub>2</sub> ·2H <sub>2</sub> O	9.75, 14.10	17.50, 19.25	1190

<sup>a</sup> Spectra taken in mull at ca. 300 K.

VII. A *Dq* value of 1000 cm<sup>-1</sup> is common for octahedral Co(II) complexes as is a nephelauxetic parameter,  $\beta$ , of 0.8–0.9. The value of  $\beta$  obtained for the cobalt complexes is much more reliable than the value obtained for the nickel complexes. In the latter case the much lower values of  $\beta$  would have indicated a considerably greater degree of covalent character in the coordinate bond than is ordinarily expected for Ni(II) complexes of this type.<sup>58</sup>

Even with this extensive amount of data, it is not possible to determine the sense of the ligand field distortion, because either axial elongation or compression would split  $\nu_1$  to approximately the same degree. Nonetheless, we believe that the distortion is more complicated than axial compression or elongation because the ligand spans *meridional* positions of the coordination polyhedron. This arrangement places the two weakest bonding atoms, the carboxylic oxygens, cis to one another. Because the positions of the intraligand bands in the cobalt complexes are the same as the bands in the nickel complexes, they are not included in Table VII.

**Electronic Spectral Data for the Fe(II) Complexes.** The electronic absorption spectrum of Fe(HPL-2(S)-val)<sub>2</sub>·2H<sub>2</sub>O is shown in Figure 7. The two bands near 9000 and 14 000 cm<sup>-1</sup> are characteristic of distorted octahedral Fe(II) and are clearly visible in the mull spectra of all five iron complexes. The bands are assigned to components of the <sup>5</sup>T<sub>2g</sub> → E<sub>g</sub> transition. The centroid of these bands corresponds to 10*Dq*.<sup>59</sup> These absorption bands and values of *Dq* are given in Table VIII. The low-intensity shoulders at ca. 17 000 and 20 000 cm<sup>-1</sup> are tentatively assigned to spin-forbidden transitions on the basis of their absence at 23 K (see Figure 7). The high-energy transitions (intraligand bands) are similar to those observed in the Ni(II) and Co(II) complexes and are not included in Table VIII.

**Infrared Spectra.** The infrared spectra of this series of complexes provides insight into the mode of bonding of the pyridoxylideneamino acid ligand to the metal ions. It is unfortunate that the pure ligands are too unstable to provide useful infrared spectra for comparison with the metal complexes. However, a generalized bonding pattern emerges by considering infrared spectral changes in a series of metal(II)

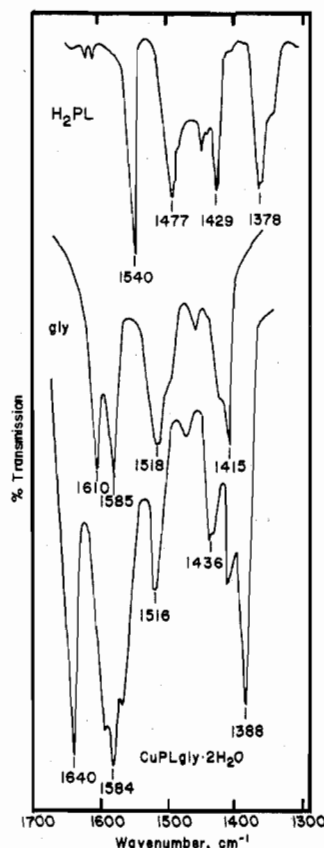
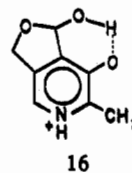


Figure 8. A comparison of the infrared spectra of H<sub>2</sub>PL, gly, and CuPLgly·2H<sub>2</sub>O in a KBr matrix.

complexes of any one of these five ligands.

A comparison of the solid-state infrared spectra of HPL, gly, and CuPLgly·2H<sub>2</sub>O in the double-bond stretching region is shown in Figure 8. The absence of a carbonyl stretching band in the spectrum of H<sub>2</sub>PL led Heinert and Martell<sup>60a</sup> to conclude that pyridoxal exists as the hemiacetal **16** in the solid



state. This structure persists in acidic or neutral aqueous solution and is still present to the extent of 75% in basic aqueous or methanolic solution.<sup>60b</sup> The free aldehyde form of H<sub>2</sub>PL shows a strong carbonyl band at 1600 cm<sup>-1</sup>. The ring-carbon phenolic oxygen stretching absorption is not observed in the spectrum of solid H<sub>2</sub>PL because of the presence of the hydrogen bond in **16**. In aqueous solution at pH 11, however, a band appears at ca. 1410 cm<sup>-1</sup> which has previously been assigned to the ring-carbon phenolate oxygen stretching absorption band.<sup>60</sup> There are four prominent bands between 1350 and 1700 cm<sup>-1</sup> in the solid-state spectrum of glycine. These absorptions have been assigned<sup>61,62</sup> as follows:  $\nu_{as}(\text{COO}^-)$ , 1610 cm<sup>-1</sup>;  $\nu_s(\text{COO}^-)$ , 1415 cm<sup>-1</sup>;  $\delta_d(\text{HN}_3^+)$ , 1585 cm<sup>-1</sup>;  $\delta_s(\text{HN}_3^+)$ , 1518 cm<sup>-1</sup>.

The formation of the Schiff base complex completely changes this portion of the spectrum (see Figure 8). Sharp bands appear at 1640, 1584, 1516, and 1388 cm<sup>-1</sup> for CuPLgly·2H<sub>2</sub>O. Similar bands are observed for the other complexes and are given in Table IX. The band near 1640 cm<sup>-1</sup> is assigned to the  $\nu(\text{CN})$  azomethine stretch. This assignment is based on similar assignments made by others<sup>63–66</sup> for related compounds. The assignment of the asymmetric



**Table IX.** Infrared Stretching Frequency Assignments in the 1700–1400-cm<sup>-1</sup> Region<sup>a</sup>

Compd	$\nu(\text{CN})$	$\nu_{\text{as}}(\text{COO}^-)$	$\nu(\text{CO}^-)$
Fe(HPLgly) <sub>2</sub>	1659	1600 sh	1500
Co(HPLgly) <sub>2</sub> ·4H <sub>2</sub> O	1650	1585	1509
Ni(HPLgly) <sub>2</sub> ·4H <sub>2</sub> O	1640 sh	1606	1524
CuPLgly·2H <sub>2</sub> O	1640	1584	1516
Mn(HPL-2(S)-ala) <sub>2</sub> ·H <sub>2</sub> O	1610	1560	1460
Fe(HPL-2(S)-ala) <sub>2</sub> ·10H <sub>2</sub> O	1625	1560	1466
Co(HPL-2(S)-ala) <sub>2</sub> ·4H <sub>2</sub> O	1653	1580 w	1462
Ni(HPL-2(S)-ala) <sub>2</sub> ·4H <sub>2</sub> O	1653	1580	1464
CuPL-DL-ala·2H <sub>2</sub> O	1638	1580	1460
Mn(HPL-2(S)-val) <sub>2</sub> ·2H <sub>2</sub> O	1655	1625	1525
Fe(HPL-DL-val) <sub>2</sub> ·2H <sub>2</sub> O	1660	1620	1518
Co(HPL-2(S)-val) <sub>2</sub> ·4H <sub>2</sub> O	1625	1600	1495
Ni(HPL-2(S)-val) <sub>2</sub> ·3.5H <sub>2</sub> O	1638	1600, 1560	1502
CuPL-2(S)-val	1650	1600	1525
Fe(HPL-2(S)-phe) <sub>2</sub> ·15H <sub>2</sub> O	1665	1600	1520
Co(HPL-2(S)-phe) <sub>2</sub> ·4H <sub>2</sub> O	1650	1605	1510
Ni(HPL-2(S)-phe) <sub>2</sub> ·3.5H <sub>2</sub> O	1632	1586	1509
CuPL-2(S)-phe·6H <sub>2</sub> O	1640	1575	1500
Mn(HPL-2(S)-trp) <sub>2</sub> ·0.5H <sub>2</sub> O	1650 sh	1610, 1595	
Fe(HPL-2(S)-trp) <sub>2</sub> ·2H <sub>2</sub> O	1660 sh	1625, 1589	1510
Co(HPL-2(S)-trp) <sub>2</sub> ·8H <sub>2</sub> O	1655 sh	1630, 1580	1505
Ni(HPL-2(S)-trp) <sub>2</sub> ·8H <sub>2</sub> O	1655 sh	1630, 1580	1505
CuPL-2(S)-trp·4H <sub>2</sub> O	1666	1610	1520

<sup>a</sup> Data given in cm<sup>-1</sup>. Abbreviations: sh = shoulder, w = weak.

carboxyl stretch,  $\nu_{\text{as}}(\text{COO}^-)$ , is based on the work of Nakamoto et al.,<sup>67</sup> Mizushima et al.,<sup>68</sup> and Sweeney et al.<sup>69</sup> The assignment of the 1516-cm<sup>-1</sup> band to the ring-carbon phenolic oxygen stretch,  $\nu(\text{CO}^-)$ , is consistent with the work of Farago et al.<sup>70</sup> on M(II) complexes of pyridoxal 5'-phosphate. The band at 1388 cm<sup>-1</sup> in the copper complexes and similar bands near 1390 cm<sup>-1</sup> in the remaining M(II) complexes of pyridoxylidene glycine are most likely due to ring-carbon stretching because of its presence in the spectrum of H<sub>2</sub>PL. It is possible that this band obscures the symmetric stretching band of the carboxylate group,  $\nu_{\text{s}}(\text{COO}^-)$ , or that one of the weak absorptions at 1436 or 1409 cm<sup>-1</sup> may be assigned to  $\nu_{\text{s}}(\text{COO}^-)$ .

Figure 9 compares the spectra of Fe(HPL-DL-ala)<sub>2</sub>·10H<sub>2</sub>O and 2(S)-ala in the same region as Figure 8. The spectrum of 2(S)-ala is similar to gly except that a band assigned to  $\delta_{\text{d}}(\text{CH}_3)$  at 1452 cm<sup>-1</sup> now appears. A set of assignments similar to those given above for  $\nu(\text{CN})$ ,  $\nu_{\text{as}}(\text{COO}^-)$ , and  $\nu(\text{CO}^-)$  for this and the remaining complexes are given in Table IX. The remaining assigned frequencies are very similar to those assigned for the metal(II) complexes of pyridoxylidene glycine and alanine. It should be noted that considerably more structure is found in the aromatic ring-carbon stretching region of the infrared spectra of the phe and trp complexes. In addition, several complexes show a splitting of the  $\nu_{\text{as}}(\text{COO}^-)$  absorption.

**Metal-Ligand Vibrations.** Percy<sup>63</sup> has assigned two bands below 600 cm<sup>-1</sup> to metal-ligand vibrations for various M-(salgly)<sub>2</sub> compounds. His assignments were based on isotopic <sup>15</sup>N band shifts which followed the Irving-Williams sequence of crystal field stabilization energies.<sup>71</sup> Such an assignment of M-L bands is valid for isostructural complexes.<sup>72,73</sup> We have been able to detect only one band in the far-infrared spectrum which behaves in this manner for the M(HPLaa)<sub>2</sub> complexes. This band occurs at ca. 400 cm<sup>-1</sup> for the isostructural series Fe(HPL-2(S)-val)<sub>2</sub>·2H<sub>2</sub>O, Co(HPL-2(S)-val)<sub>2</sub>·4H<sub>2</sub>O and Ni(HPL-2(S)-val)<sub>2</sub>·3.5H<sub>2</sub>O. The shift is ca. +6 cm<sup>-1</sup> in going from the Ni to the Co complex and ca. +7 cm<sup>-1</sup> in going from the Co to the Fe complex. It is unfortunate that the other series of isostructural compounds reported here do not show such behavior. This difficulty may be traced to the fact that numerous low-energy bands occur in the spectra of these materials making such small shifts hard to observe. Because no free ligand spectra are available for comparison

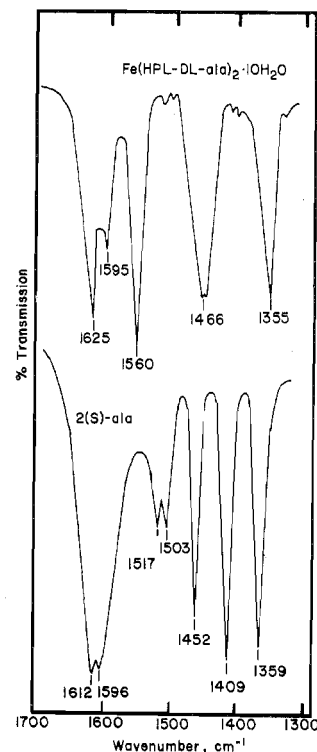


**Figure 9.** A comparison of the infrared spectra of 2(S)-ala and Fe(HPL-DL-ala)<sub>2</sub>·10H<sub>2</sub>O in a KBr matrix.

it is not possible to assign any band shifts upon complex formation. We have prepared the <sup>58</sup>Ni and <sup>62</sup>Ni complexes of HPL-2(S)-val but did not observe any shifts that could be attributed to the isotope mass effect.

### Conclusions

The magnetic and electronic spectral properties of the Mn(II), Fe(II), Co(II), and Ni(II) complexes of the pyridoxylideneamino acids discussed in this paper are consistent with a distorted octahedral coordination geometry. Related ligands with the same set of donor atoms as the pyridoxylideneamino acids form similar octahedral complexes as in the case of K[Fe(salaa)<sub>2</sub>],<sup>74</sup> [Fe(H<sub>2</sub>O)<sub>6</sub>][Fe(salgly)<sub>2</sub>]<sub>2</sub>·2H<sub>2</sub>O,<sup>75</sup> and [Co(H<sub>2</sub>O)<sub>6</sub>][Co(salgly)<sub>2</sub>]<sub>2</sub>·2H<sub>2</sub>O.<sup>75</sup> In general, salicylideneamino acid ligands form bis-complexes of the type [M(salaa)<sub>2</sub>]<sup>-</sup>. In all of these complexes the metal is trivalent. In comparison, six-coordinate divalent complexes of the type [M(salaa)(H<sub>2</sub>O)<sub>2</sub>]<sub>2</sub> are obtained only through bridging carboxylate oxygen atoms.<sup>63</sup> In contrast, the divalent metal complexes of the pyridoxylideneamines form M(PLamine)<sub>2</sub> complexes,<sup>76-80</sup> where PLamine is the Schiff base derived from pyridoxal and a primary aliphatic amine, or M(HPLaa)<sub>2</sub> complexes, where HPLaa are the Schiff bases discussed in this paper. Yamada et al.<sup>78</sup> have prepared several Co(III) complexes of the type Co(PLamine)<sub>3</sub>. These materials are diamagnetic and have electronic properties consistent with low-spin Co(III). On the other hand we have observed that the PLaa<sup>2-</sup> ligands bind to Fe(III) forming mono complexes of the general type [Fe(PLaa)]<sup>+</sup>.<sup>79</sup> This interesting coordination behavior at once implies that complexes of simple salicylideneamino acids are not good models for pyridoxylideneamino acid complexes. This conclusion supports the fact that salicylaldehyde is not an effective transamination substrate.<sup>80,81</sup> The dissimilarity between the coordination properties of salicylideneamino acid ligands and those of the pyridoxylideneamino acid ligands may be traced to the presence of the basic pyridine nitrogen in the latter compounds.

The magnetic and electronic spectral properties of the Cu(II) complexes discussed herein are consistent with five-

coordination. This coordination number has been observed<sup>82</sup> for the square-pyramidal complex,  $[\text{Cu}(\text{salgly})(\text{H}_2\text{O})]\cdot 0.5\text{H}_2\text{O}$ , in which the copper is weakly bonded to a carboxylate oxygen of an adjacent molecule. The results reported in this paper are also consistent with the published single-crystal x-ray results of Willstadter et al.,<sup>29</sup> Cutfield et al.,<sup>30</sup> and Capasso et al.<sup>31</sup>

It is interesting that  $\text{Cu}^{2+}$  is a much more effective catalyst for many of the reactions involving pyridoxal than  $\text{Co}^{2+}$ ,  $\text{Ni}^{2+}$ , or  $\text{Zn}^{2+}$ . This relative effect may be understood in terms of the coordination chemistry of these ions. Whereas  $\text{Co}^{2+}$ ,  $\text{Ni}^{2+}$ , and  $\text{Zn}^{2+}$  prefer octahedral coordination,  $\text{Cu}^{2+}$  is known to form complexes of lower coordination number.<sup>46</sup> The effectiveness of  $\text{Cu}^{2+}$  as a catalyst may be directly related to its ability to form mono complexes of the type  $\text{Cu}(\text{PLaa})$  in which the planarity of the ligand is both sterically and electronically favored, thereby facilitating electron delocalization and thus lowering the energy of the corresponding intermediate. On the other hand, the relative ineffectiveness of  $\text{Co}^{2+}$ ,  $\text{Ni}^{2+}$ , and  $\text{Zn}^{2+}$  may be due to their preference for octahedral coordination which does not permit an extensive  $\pi$  delocalization because of steric crowding in the coordination sphere which disrupts the planar structure of the ligand. The observation<sup>14</sup> that  $\text{Fe}^{2+}$  is nearly as effective as  $\text{Fe}^{3+}$  in transamination and deamination reactions is puzzling because we have observed<sup>79</sup> that  $\text{Fe}^{3+}$  forms complexes with the pyridoxylideneamino acids of the type  $\text{Fe}(\text{PLaa})^+$ . If the rate of metal ion catalyzed pyridoxal reactions depends on the nature of the complex then  $\text{Fe}^{2+}$  and  $\text{Fe}^{3+}$  mediated reactions should show considerably different rates. We have prepared a number of reaction mixtures of pyridoxamine,  $\alpha$ -ketoglutarate, and  $\text{FeCl}_3$  or  $\text{FeCl}_2$  which are identical in composition with the mixtures used by Longenecker and Snell<sup>14</sup> in their rate studies. When these mixtures were heated to 100 °C in air, the initially green mixture containing  $\text{FeCl}_2$  changed within 2 min to a red solution which was identical with the solution containing  $\text{FeCl}_3$ . An analogous solution of  $\text{FeCl}_2$  heated to 100 °C under an inert atmosphere remained green. Thus apparently oxygen is able to oxidize the  $\text{FeCl}_2$  to  $\text{FeCl}_3$  under the conditions of this experiment. These results indicate that, under the experimental conditions used by Longenecker and Snell,<sup>14</sup>  $\text{Fe}^{2+}$  was oxidized to  $\text{Fe}^{3+}$  thereby increasing the apparent rates of transamination and deamination ascribed to  $\text{Fe}^{2+}$ .

**Acknowledgment.** It is a pleasure to acknowledge the helpful discussions which were held with Dr. L. M. Nicholson. The financial assistance of the National Science Foundation through Grants GP-8653 and CHE 75-20417 is gratefully appreciated. A Department of Defense Themis Grant made possible the purchase of components for the Mössbauer spectrometer.

**Registry No.**  $\text{CuPLgly}$ , 63569-26-6;  $\text{CuPL-2(S)-ala}$ , 63569-27-7;  $\text{CuPL-2(S)-val}$ , 63569-28-8;  $\text{CuPL-2(S)-phe}$ , 63569-29-9;  $\text{CuPL-2(S)-trp}$ , 63569-30-2;  $\text{Ni(HPLgly)}_2$ , 63598-82-3;  $\text{Ni(HPL-2(S)-ala)}_2$ , 63598-83-4;  $\text{Ni(HPL-2(S)-val)}_2$ , 63598-84-5;  $\text{Ni(HPL-2(S)-phe)}_2$ , 63569-31-3;  $\text{Ni(HPL-2(S)-trp)}_2$ , 63569-32-4;  $\text{Co(HPLgly)}_2$ , 63598-85-6;  $\text{Co(HPL-2(S)-ala)}_2$ , 63569-33-5;  $\text{Co(HPL-2(S)-val)}_2$ , 63569-34-6;  $\text{Co(HPL-2(S)-phe)}_2$ , 63569-35-7;  $\text{Co(HPL-2(S)-trp)}_2$ , 63569-36-8;  $\text{Fe(HPLgly)}_2$ , 63569-37-9;  $\text{Fe(HPL-DL-ala)}_2$ , 63569-38-0;  $\text{Fe(HPL-DL-val)}_2$ , 63569-39-1;  $\text{Fe(HPL-2(S)-phe)}_2$ , 63569-40-4;  $\text{Fe(HPL-2(S)-trp)}_2$ , 63569-41-5;  $\text{Mn(HPL-2(S)-ala)}_2$ , 63569-42-6;  $\text{Mn(HPL-2(S)-val)}_2$ , 63569-43-7;  $\text{Mn(HPL-2(S)-trp)}_2$ , 63569-44-8;  $\text{Fe(HPL-2(S)-ala)}_2$ , 63598-86-7;  $\text{Fe(HPL-2(S)-val)}_2$ , 63598-87-8;  $\text{CuPL-DL-ala}$ , 63569-45-9;  $\text{H}_2\text{PL}$ , 66-72-8; glycine, 56-40-6; 2(S)-alanine, 56-41-7; DL-alanine, 302-72-7;  $\text{H}_2\text{PL}\cdot\text{HCl}$ , 65-22-5; 2(S)-valine, 72-18-4; 2(S)-trp, 73-22-3.

**Supplementary Material Available:** Listings of elemental analysis, Table I, x-ray powder diffraction data, Table II, and magnetic data at various temperatures, Table IIIB (8 pages). Ordering information

is given on any current masthead page.

## References and Notes

- (1) A. E. Braunstein, *Enzymologia*, **7**, 25 (1939).
- (2) P. P. Cohen, *Biochem. J.*, **33**, 1478 (1939).
- (3) E. E. Snell, *J. Am. Chem. Soc.*, **67**, 194 (1945).
- (4) D. E. Metzler, M. Ikawa, and E. E. Snell, *J. Am. Chem. Soc.*, **76**, 648 (1954).
- (5) B. M. Guirard and E. E. Snell, *J. Am. Chem. Soc.*, **76**, 4745 (1954).
- (6) M. Ikawa and E. E. Snell, *J. Am. Chem. Soc.*, **76**, 4900 (1954).
- (7) D. L. Leussing and D. C. Shultz, *J. Am. Chem. Soc.*, **86**, 4846 (1964).
- (8) J. W. Thanassi, *Biochemistry*, **9**, 525 (1970).
- (9) T. Pfeuffer, J. Ehrlich, and E. Helmreich, *Biochemistry*, **11**, 2125 (1972).
- (10) A. Hogberg-Raibaud, O. Raibaud, and M. E. Goldberg, *J. Biol. Chem.*, **250**, 3352 (1975).
- (11) E. E. Snell, P. M. Fasella, A. Braunstein, and A. Rossi-Fanelli, "Chemical and Biological Aspects of Pyridoxal Catalysis", Macmillan, New York, N.Y., 1963.
- (12) T. C. Bruice and S. J. Benkovic, "Bio-Organic Mechanisms", Vol. 2, W. A. Benjamin, New York, N.Y., 1966.
- (13) D. E. Metzler and E. E. Snell, *J. Am. Chem. Soc.*, **74**, 979 (1952).
- (14) J. B. Longenecker and E. E. Snell, *J. Am. Chem. Soc.*, **79**, 142 (1957).
- (15) A. E. Braunstein, *Adv. Protein Chem.*, **3**, 1 (1947).
- (16) M. E. Farago and T. Matthews, *J. Chem. Soc. A*, 609 (1969).
- (17) P. Pfeiffer, W. Offermann, and J. Werner, *J. Prakt. Chem.*, **159**, 313 (1942).
- (18) H. N. Christensen and T. R. Riggs, *J. Biol. Chem.*, **220**, 265 (1956).
- (19) H. N. Christensen and S. Collins, *J. Biol. Chem.*, **220**, 279 (1956).
- (20) H. N. Christensen, *Biochem. Prep.*, **6**, 612 (1957).
- (21) H. N. Christensen, *J. Am. Chem. Soc.*, **79**, 4073 (1957).
- (22) H. N. Christensen, *J. Am. Chem. Soc.*, **80**, 2305 (1958).
- (23) J. Baddiley, *Nature (London)*, **170**, 711 (1952).
- (24) E. H. Abbott and A. E. Martell, *J. Am. Chem. Soc.*, **91**, 6866 (1969).
- (25) E. H. Abbott and A. E. Martell, *J. Am. Chem. Soc.*, **92**, 5845 (1970).
- (26) O. A. Gansow and R. H. Holm, *J. Am. Chem. Soc.*, **90**, 5629 (1968).
- (27) O. A. Gansow and R. H. Holm, *J. Am. Chem. Soc.*, **91**, 573 (1969).
- (28) A. E. Martell and A. F. Eidson, *Bioinorg. Chem.*, **4**, 277 (1975).
- (29) E. Willstadter, T. A. Hamor, and J. L. Hoard, *J. Am. Chem. Soc.*, **85**, 1205 (1963).
- (30) J. F. Cutfield, D. Hall, and T. N. Waters, *Chem. Commun.*, 785 (1967).
- (31) S. Capasso, F. Giordano, C. Mattia, L. Mazzarella, and A. Ripamonti, *J. Chem. Soc., Dalton Trans.*, 2228 (1974).
- (32) R. H. Holm, "Inorganic Biochemistry", G. L. Eichhorn, Ed., Elsevier, New York, N.Y., 1973, Chapter 31, p. 1137.
- (33) E. L. Eliel, "The Stereochemistry of Carbon Compounds", McGraw-Hill, New York, N.Y., 1962, p. 92ff.
- (34) Manufactured by Air Products Corp., Allentown, Pa.
- (35) Kel-F 90 is a registered trademark of the 3M Co.
- (36) J. T. Wroblewski and G. J. Long, *Appl. Spectrosc.*, **31**, 177 (1977).
- (37) P. E. Rakita, S. J. Kopperl, and J. P. Fackler, Jr., *J. Inorg. Nucl. Chem.*, **30**, 2139 (1968).
- (38) B. N. Figgis and R. S. Nyholm, *J. Chem. Soc.*, 4190 (1958).
- (39) F. E. Mabbs and D. J. Machin, "Magnetism and Transition Metal Complexes", Chapman and Hall, London, 1973, p. 5.
- (40) R. M. Zacharius and E. A. Talley, *Anal. Chem.*, **34**, 1551 (1962).
- (41) D. E. Metzler and E. E. Snell, *J. Am. Chem. Soc.*, **74**, 979 (1952).
- (42) Supplementary material.
- (43) A common problem encountered with the analysis of compounds containing large amounts of lattice water is that the water may be lost by evaporation during CHN analysis. This specifically manifests itself in the low values for hydrogen for these compounds. The hydration number for these materials is calculated on the basis of best fit empirical formula to carbon, nitrogen, and metal analyses. Several other workers have reported this difficulty.<sup>28,30</sup>
- (44) B. N. Figgis, "Introduction to Ligand Field Theory", Interscience, New York, N.Y., 1966, p. 278.
- (45) A. Earnshaw, "Introduction to Magnetochemistry", Academic Press, New York, N.Y., 1968.
- (46) B. J. Hathaway, "Essays in Chemistry", Vol. 2, J. N. Bradley, R. D. Gillard, and R. F. Hudson, Ed., Academic Press, New York, N.Y., 1971, p. 61.
- (47) H. L. Schläfer and G. Gliemann, "Basic Principles of Ligand-Field Theory", Wiley-Interscience, New York, N.Y., 1969.
- (48) F. A. Cotton and G. Wilkinson, "Advanced Inorganic Chemistry", 2nd ed, Interscience, New York, N.Y., 1962, p. 836ff.
- (49) H. Frauenfelder, "The Mössbauer Effect", W. A. Benjamin, New York, N.Y., 1962.
- (50) L. R. Walker, G. K. Wertheim, and V. Jaccarino, *Phys. Rev. Lett.*, **6**, 98 (1961).
- (51) L. Davis, F. Roddy, and D. E. Metzler, *J. Am. Chem. Soc.*, **83**, 127 (1961).
- (52) A. C. Braithwaite, P. E. Wright, and T. N. Waters, *J. Inorg. Nucl. Chem.*, **37**, 1669 (1975).
- (53) J. Ferguson, *Prog. Inorg. Chem.*, **12**, 159 (1970).
- (54) E. König, *Struct. Bonding (Berlin)*, **9**, 175 (1971).
- (55) J. S. Griffith, "The Theory of Transition-Metal Ions", Cambridge University Press, Cambridge, 1964, p. 437.
- (56) C. K. Jørgensen, "Absorption Spectra and Chemical Bonding in Complexes", Pergamon Press, Oxford, 1964, p. 134.
- (57) D. S. McClure, "Treatise on Solid State Chemistry", Vol. 2, N. B. Hannay, Ed., Plenum Press, New York, N.Y., 1975.

- (58) C. K. Jørgensen, "Modern Aspects of Ligand-Field Theory", American-Elsevier, New York, N.Y., 1971.
- (59) Reference 44, p 225.
- (60) (a) D. Heinert and A. E. Martell, *J. Am. Chem. Soc.*, **81**, 3933 (1959); (b) C. M. Harris, R. J. Johnson, and D. E. Metzler, *Biochim. Biophys. Acta*, **421**, 181 (1976).
- (61) M. Tsuboi, T. Onishi, I. Nakagawa, T. Shimanouchi, and S. Mizushima, *Spectrochim. Acta*, **12**, 253 (1958).
- (62) K. Fukushima, T. Onishi, T. Shimanouchi, and S. Mizushima, *Spectrochim. Acta*, **15**, 236 (1959).
- (63) G. C. Percy, *J. Inorg. Nucl. Chem.*, **37**, 2071 (1975).
- (64) H. A. O. Hill and N. Zarb-Adami, *J. Inorg. Nucl. Chem.*, **37**, 2443 (1975).
- (65) G. C. Percy and D. A. Thornton, *J. Inorg. Nucl. Chem.*, **34**, 3369 (1972).
- (66) E. P. Dudek and G. Dudek, *Inorg. Nucl. Chem. Lett.*, **3**, 241 (1967).
- (67) K. Nakamoto, Y. Morimoto, and A. E. Martell, *J. Am. Chem. Soc.*, **83**, 4528 (1961).
- (68) S. Mizushima, I. Ichishima, I. Nakagawa, and J. V. Quagliano, *J. Phys. Chem.*, **59**, 293 (1955).
- (69) D. M. Sweeny, S. Mizushima, and J. V. Quagliano, *J. Am. Chem. Soc.*, **77**, 6521 (1955).
- (70) M. E. Farago, M. M. McMillan, and S. S. Sabir, *Inorg. Chim. Acta*, **14**, 207 (1975).
- (71) L. G. Hulett and D. A. Thornton, *Spectrochim. Acta, Part A*, **27**, 2089 (1971).
- (72) K. Nakamoto, "Infrared Spectra of Inorganic and Coordination Compounds", Wiley, New York, N.Y., 1970.
- (73) G. S. Shephard and D. A. Thornton, *J. Mol. Struct.*, **16**, 321 (1973).
- (74) R. C. Burrows and J. C. Bailar, *J. Am. Chem. Soc.*, **88**, 4150 (1966).
- (75) F. T. Helm, Ph.D. Dissertation, Georgia Institute of Technology, 1973.
- (76) S. Yamada, Y. Kuge, and T. Yamayoshi, *Inorg. Chim. Acta*, **9**, 29 (1974).
- (77) S. Yamada, H. Kuma, and K. Yamanouchi, *Inorg. Chim. Acta*, **10**, 151 (1974).
- (78) S. Yamada, Y. Kuge, T. Yamayoshi, and H. Kuma, *Inorg. Chim. Acta*, **11**, 253 (1974).
- (79) J. T. Wroblewski and G. J. Long, in preparation.
- (80) M. Ando and S. Emoto, *Bull. Chem. Soc. Jpn.*, **42**, 2628 (1969).
- (81) M. Ando and S. Emoto, *Bull. Chem. Soc. Jpn.*, **48**, 1655 (1975).
- (82) T. Ueki, T. Ashida, Y. Sasada, and M. Kakudo, *Acta Crystallogr.*, **22**, 870 (1967).

Contribution from the Department of Chemistry, Wayne State University, Detroit, Michigan 48202, and Departamento de Química, Universidad Técnica del Estado, Santiago, Chile

## Photostimulated Solvolytic Reactions of a Macrocyclic Copper Complex<sup>1a</sup>

GUILLERMO J. FERRAUDI\*<sup>1b</sup> and JOHN F. ENDICOTT<sup>1c</sup>

Received January 18, 1977

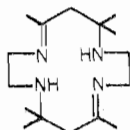
AIC70041T

The photochemical behavior of  $\text{Cu}([14]\text{dieneN}_4)^{2+}$  was studied under various experimental conditions for excitations in the region of the charge-transfer transitions. Two processes, ligand hydrolysis in aqueous solutions and formation of reduced copper(I) species in methanol, were detected as the photochemical modes of reaction for this ion. A ketone-amine intermediate product was characterized in the aqueous photoreaction and a precursor, possibly a carbinolamine species ( $t_{1/2} \approx 0.03$  s), was observed by means of flash photolysis. The slow formation of Cu(I) was observed in neat methanol by a second-order reaction ( $k = 2.2 \times 10^4 \text{ M}^{-1} \text{ s}^{-1}$ ). A mechanism based on a common precursor with ligand and metal reaction centers was proposed.

### Introduction

Since copper complexes often serve as labile mediators of redox reactions, one might expect photoredox reactions of copper complexes to be of some potential significance. Yet there have been few systematic studies.<sup>2-7</sup> Among the recent studies, those of Davis and Stevenson<sup>2</sup> and of Kutal and co-workers<sup>3</sup> are of interest in that they attempt to use copper complexes to produce the conversion of solar to storable chemical energy. Several years ago, Wehry proposed a direct photooxidation of solvent species, water or methanol, by copper(II) phenanthroline complexes<sup>4</sup> while Lintvedt and DeGraaf and their co-workers had found evidence that photoredox processes in other copper chelates involved production of radical ligand species, followed by often complex and rapid radical reactions with solvent and/or substrate.<sup>5,6</sup>

In this report we describe our photochemical studies of  $\text{Cu}([14]\text{dieneN}_4)^{2+}$ .<sup>8</sup> It seemed possible that the macrocyclic [14]dieneN<sub>4</sub> ligand would be stable to the complexities in-



[14] dieneN<sub>4</sub>

roduced by radical reactions of more labile ligand systems and that one might be enabled to observe simple intermolecular reactions between the excited copper complex and solvent species.

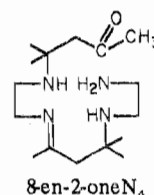
### Experimental Section

Continuous irradiations were performed using either resonance emission lines of Philips Zn, Cd, and Hg spectral lamps or spectral bands from a medium-pressure Hg lamp (1 kW). The source was

arranged on an optical bench with a collimating lens system, slits, a water filter plus the interference filter, and sample cell as appropriate to the experiment. Ferrioxalate<sup>9</sup> and uranyl oxalate<sup>10</sup> were used as the primary actinometric references. The light intensity for a given source was checked frequently with  $\text{Co}(\text{NH}_3)_5\text{Cl}^{2+}$  or  $\text{Co}(\text{NH}_3)_5\text{Br}^{2+}$ .<sup>11</sup>

Solutions were deaerated either with streams of nitrogen ( $\text{Cr}^{2+}$  scrubbed) or by four freeze-pump-thaw cycles. The latter procedure was used for determinations of the quantum yields in methanolic solutions owing to the reactivity of the copper(I) product with dioxygen. An analytical procedure for this species was developed in order to minimize losses. Oxidation of the cuprous species in the photolyte was carried out with a vacuum deaerated solution of  $\text{Fe}^{3+}$  ( $10^{-4}$  M) placed in a detachable side arm of the reaction cell. Solutions were mixed under vacuum, and the  $\text{Fe}^{2+}$  was analyzed with 1,10-phenanthroline.<sup>12</sup> Unphotolyzed solutions, handled in the same manner, were used as references. Copper(II) was analyzed with rubeanhydric acid (ditizone).<sup>13</sup> Tests for primary amines, methyl ketones, and formaldehyde were performed according to literature descriptions.<sup>14</sup> The search for pseudo-macrocyclic complexes was carried out with appropriate  $\text{Cu}^{2+}(\text{aq})$  reagents in acid medium (0.1–0.05 M  $\text{I}^-$  or ditizone).

Flash irradiations<sup>15</sup> of  $\text{Cu}([14]\text{dieneN}_4)^{2+}$  in methanolic media were performed on solutions degassed by four freeze-pump-thaw cycles. Transfer to the flash photolysis cell was carried out under an argon atmosphere in a gas-tight apparatus. Aqueous solutions were liberated of oxygen with nitrogen (scrubbed in towers filled with chromous solutions). Literature procedures were used for the synthesis of  $[\text{Cu}([14]\text{dieneN}_4)](\text{ClO}_4)_2$ <sup>16</sup> and  $[\text{Cu}(8\text{-en-2-oneN}_4)](\text{ClO}_4)_2$ .<sup>8,17</sup>



8-en-2-oneN<sub>4</sub>